This is to certify that the

thesis entitled
DESIGN AND CHARACTERIZATION OF A

FLOW REVERSAL/FLOW RECYCLE

CONTINUOUS FLOW ANALYSIS SYSTEM
presented by

Edwin B. Townsend IV

has been accepted towards fulfillment
of the requirements for

MS degree in Chemistry

Major professor

Date 4/29/91

DESIGN AND CHARACTERIZATION OF A FLOW REVERSAL/FLOW RECYCLE CONTINUOUS FLOW ANALYSIS SYSTEM

by

EDWIN B. TOWNSEND IV

A DISSERTATION

Submitted to
Michigan State University
in partial fulfillment of the requirements
for the degree of

MASTER OF SCIENCE

Department of Chemistry

1991

Abstract

DESIGN AND CHARACTERIZATION OF A FLOW REVERSAL/FLOW RECYCLE CONTINUOUS FLOW ANALYSIS SYSTEM

by

Edwin B. Townsend IV

A continuous flow analysis system that is capable of performing either flow reversals or flow recycles has been constructed. The key components are two 6 port switching valves, which are used to allow the flowing analytical stream to be either reversed or recycled following the passage of sample through the flow cell and the subsequent detection of a peak by the detector. An interface has been developed that allows for complete computer control of both the valve switching and the data acquisition after the operator enters experimental parameters.

The new system is characterized through the use of a series of photometric determinations. Both peak area and peak height are used to characterize the sample peaks, and the variation in those measurements caused by the number of reversals or recycles is determined to be minimal. The analytical utility of flow reversals and flow recycles is demonstrated by the generation of standard curves and the determination of nitrite. Finally, a slow kinetic determination is chosen and compared with an alternate photometric detection method to demonstrate the usefulness of reversals and/or recycles.

DEDICATION

I'd like to take this opportunity to dedicate this thesis to my brother, Kevin. He is currently serving aboard the U.S.S. Biddle CG-34, and was in the Red Sea during the Gulf War. He is brave enough to be doing something that I could never do, and I have the utter most respect and admiration for him. Beef, God Bless you and I'm very thankful that you came home safely.

ACKNOWLEDGEMENTS

I would like to thank Professor Stanley Couch for his guidance, friendship, and faith in me during the course of this research. Without his belief in me, I would probably not be writing this thesis right now.

I would also like to thank my wife, Maria, for her support and unbridled faith in me. Without her, my life would just be on one even, unexciting, uneventful keel.

Many more thanks to the members of the Crouch group. Kris, SVM, BQ, Odie, DT, Larry, and Dave S. all make lab a great place to work. I hope that I have been able to make it the same for them. Also, thanks to our "honorary" group member and resident QuickBasic expert, Eric Hemenway. Without his help, the computer code might not have ever gotten off the ground.

I'd also like to thank all the others in "group". They include Knurt, Tracy, Gary, Gilbey, Berly, Laura, Jason, Sue, Mary, Mark, Drs. Light & Wahl-Light, and Dave G., among others. You guys make grad school a real experience.

TABLE OF CONTENTS

LIST OF TABLES

LIST OF FIGURES

Chapter 1

Historical, Theoretical, and Literature Introduction to Continuous Flow Analysis

A. Overview

Flow analysis can roughly be defined as the transport of a sample from the start of sampling until reaching waste (1). In between the start and the finish, several events may occur. These events include, but are not restricted to, mixing, reacting, separating, and/or detecting one or more analytes in the sample. Two well-known subdivisions of flow analysis are Air-segmented Continuous Flow Analysis (CFA) and Flow Injection Analysis (FIA). Air-segmented continuous flow analysis was first conceptualized by Leonard Skeggs (2,3) in 1957 and then developed commercially by the Technicon Corporation as the AutoAnalyzer (Technicon Instruments, Tarrytown, NY). Flow Injection Analysis was developed nearly simultaneously in the 1970's by the pair of Jaromir Ruzicka and Elo Hansen (4) in Denmark and by Kent Stewart (5) in the United States. The major physical quality differentiating FIA from CFA is the air bubble that is introduced into the flowing stream in CFA, while FIA is thought of as unsegmented or nonsegmented continuous flow analysis. This physical difference gives each system unique properties, as well as offering advantages and disadvantages over the other.

Since this investigation deals primarily with continuous flow systems, only historical information, theory, and pertinent applications for CFA are

discussed. However, necessary FIA information and comparisons are presented whenever appropriate.

B. History of Continuous Flow Analysis

1. Introduction

Air-segmented continuous flow analysis was invented by Skeggs (2) and commercially marketed by the Technicon Corporation. In an effort to automate batch analysis, Skeggs, in the early 1950's, decided to forgo the conventional idea of developing an instrument that included traditional analytical tools such as test tubes and pipets, and instead to began working on a novel idea to perform sequential batch analysis based upon a continuously flowing stream. This continuously flowing stream would be contained in interconnected, small diameter tubes called a manifold. Initially, CFA was developed to satisfy the demands for more clinical laboratory determinations, and in fact, Skeggs found CFA useful for such things as removing interferences in clinical assays or for improving clinical dialysis. However, his most significant development in CFA was "the bubble". Skeggs had found that the performance of his CFA system was being significantly handicapped because of the intermixing of samples as they passed through the reaction manifold. He solved this intermixing problems by inserting air bubbles, at regular intervals, into the flowing stream.

Thus, Air-segmented Continuous Flow analysis was born. Because a very detailed account of the development of CFA by Skeggs and the resulting commercialization of CFA by the Technicon Corporation is given in a recent article (6), I will not go into great detail about every

development, but instead will highlight those which significantly increased the capability, performance, or versatility of CFA systems.

2. The AutoAnalyzer I

The first patent in CFA was issued to Skeggs in 1957 (3). That same year, Technicon sold a single-channel CFA system known as the AutoAnalyzer (AAI). This system first sold in 1957 differs little in basic components when compared to the current systems of today. The differences that do exist are due to the quality of equipment and to computerization. In 1957, dependable peristaltic pumps, durable, inert pump tubing, mixing coils, and specialized fittings were not available. For example, in 1957, the inner diameter of mixing coils, fittings, and flow cells was 3 mm, and flow rates were around 10-15 mL/min, which resulted in low sample throughput. Sample interaction of greater than 10% was prevalent, caused mostly by sample residues adhering to the walls of the tubing and the procedure of using air plugs between samples, instead of the analyte-free wash that is currently used (7). The precision of determinations was poor due to variations in the volume of analyte sample aspirated (7). Severe fluctuations in the flow rate and in the volume of the analytical stream also exist because of the compressibility of the air segments as they passed under the pump rollers (8). Sharp peaks without flat tops were also the norm because of the large dead volumes of the debubbler and flow cell (8). Improvements in the sampler, debubbler, and flow cells all took place through the early 1960's to enhance the performance of the commercial system.

3. Enhancing the AutoAnalyzer I

The next major change in the AAI was the double-crook sampler (9). It resulted in a relatively constant delivery of liquid and air into the analytical cartridge, because it reversed the role of the sample and air delivery pump tubes during the sample and wash cycle. Also at this time, the problem of poor wash in the tubing between the sampler and the analytical cartridge was addressed by de Jong (10). This problem was solved by implementing a much more rapid mechanism to cycle the sample withdrawal tube between samples and by constantly renewing the the supply of analyte-free wash. Also an improved, low volume flow cell and a more efficient debubbler were introduced (11).

4. SMA 12/30

In 1965, Technicon introduced the SMA 12/30 (12), which was a 12 channel version of an analyzer developed in 1964 (13). This system was originally developed by Skeggs and Hochstrasser and could perform eight clinical determinations in parallel, with a rate of 20 samples/hour. It included a single light source and a photometric detector; these were multiplexed to eight flow cells on a stage. The steady state signals were achieved in sequential 20-sec intervals.

5. Second Generation Systems

Second-generation hardware was introduced in 1967 (14). Technicon produced the SMA 12/60 clinical analyzer, which determined 12 samples in parallel at a rate of 60 samples/hour (60 x 12 = 720 actual measurements per hour). This new analyzer contained several key, new hardware developments. The first came about when it was realized that uniform

proportioning could be achieved with peristaltic pumps, provided that gas segments were added in phase with pump pulsations (15). Another major enhancement included decreasing the internal diameter of the analytical tubing, mixing coils, and tees, to 2 mm. This reduction in size also decreased the flow rate of the stream to 2.5 mL/min. Because of the lower volume of sample coming through the flow cell and its debubbler, the wash improved significantly (14). As a result, the SMA 12/60 was a major improvement over the first generation systems in terms of precision, analysis time, and cost. All of these new features were introduced in 1970, in Technicons' AutoAnalyzer II (AAII), which was quickly accepted as the industry standard (16).

6. Third Generation Systems

Third-generation hardware appeared in 1972 (17,18) in the form of Technicon's 20-channel SMAC clinical analyzer. It was in this generation of instrumentation that CFA really matured. It involved pumps, mixing tees, flow cells, and pump tubing that were further miniaturized, with flow tubing reaching an internal diameter of 1 mm. These changes led to improvements in flow rate (< 1 mL/min) and segmentation frequency (from 30 bubbles/min to 90 bubbles/min). Also, dispersion occurring in unsegmented areas of the CFA system, such as the area between the pump and the mixing tee, was reduced by using both the pecked sampling technique and bubble-through flow cells (18). Fiber optics and interference filters were introduced at this time and used to multiplex the large number of flow cells to a single detector. Artifacts from air-segments were removed with computer technology, and data were taken only from the flat region of a peak. These changes resulted in a high sample frequency (150

samples/hour), low-dispersion system. The demands on sample and reagent amounts were also decreased. Theory (19,20) predicts the possibility of building lower dispersion systems with smaller tubing, lower flow rates, and increased segmentation frequencies. However, the resultant gains in speed and decreases in sample and reagent consumption would not offset the technical difficulties and costs associated with further miniaturization (21). As a result, any new CFA hardware development past third generation is not foreseen. What will improve is data analysis and manipulation techniques, and any new systems being developed will be designed and constructed using existing technology.

It should also be noted here that "in-house" third-generation systems were also being developed at this time. These systems were being built first by Neeley *et al.* (22-25) and then later by Patton and Couch (26-28). The CFA system designed by Patton (27), and later marketed commercially by Alpkem as the Rapid Flow Analyzer, serves as the model for the system to be developed and described in this thesis. Details of the system are discussed later in Chapter 2.

C. Theory of Continuous Flow Analysis

1. Introduction

A generalized CFA system is shown in Figure 1-1 (a typical set-up). It operates in this manner. Samples are aspirated into flow tubing, pumped through the tubing into the mixing tee, from the mixing tee through a mixing coil, and then through a detector to waste. The air bubble artifact can be removed in two ways, either before or after the sample detection. If the bubble is to be removed prior to detection, a

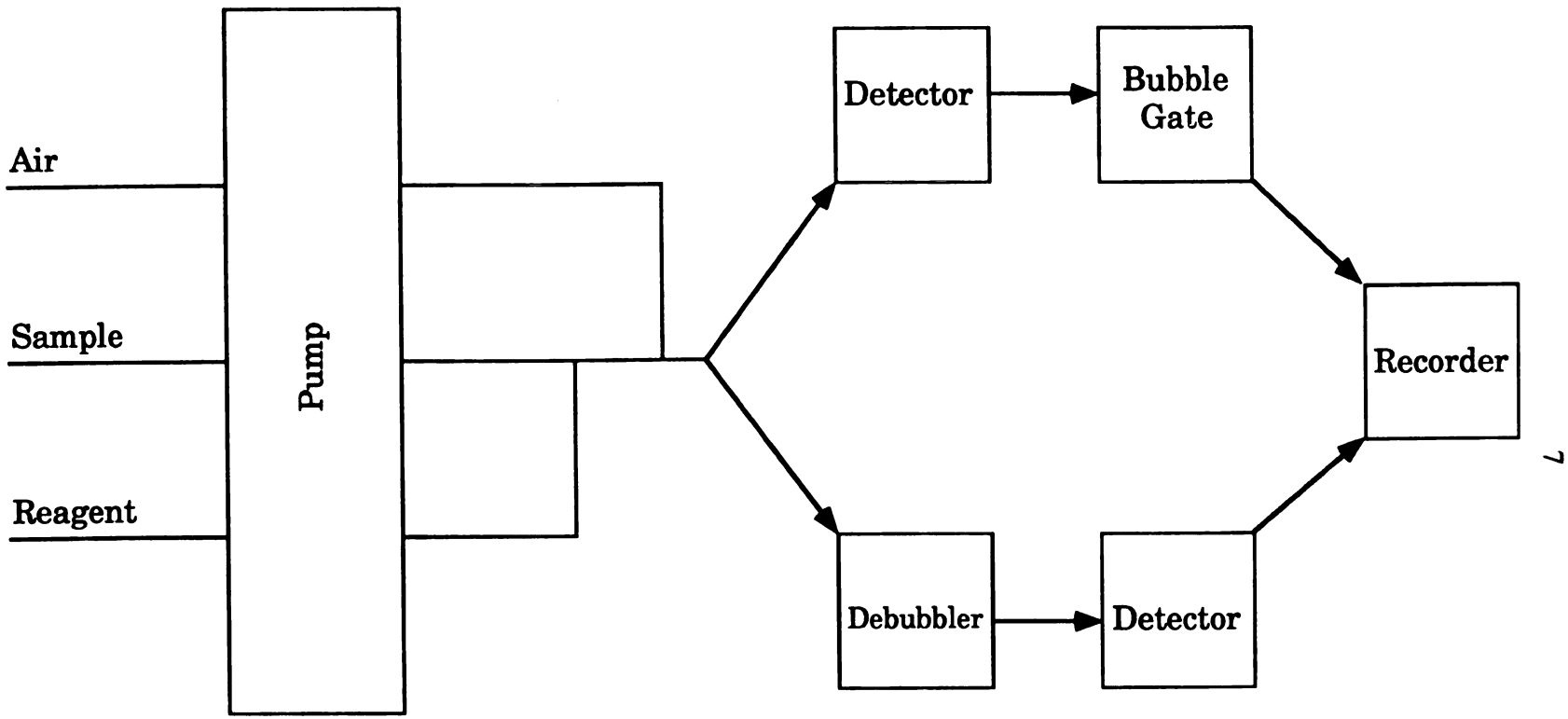

Figure 1-1. A generalized diagram of a typical CFA set-up.

debubbler is used. This piece of equipment looks physically like an "F"; the sample is pumped through to the detector while the air bubble is diverted to waste. The second alternative is to remove the signal from the air bubble electronically after the detector by using a bubblegate. An analyte-free wash solution is aspirated between samples. The volume of sample drawn into the manifold is dependent on the residence time of the tube aspirating the sample and the flow rate of the tube. Both sample and wash slugs are segmented with air bubbles as they enter the mixing tee. After the measurement has been made, the sample is pumped to waste.

The theory of CFA is well understood, as evidenced in articles by Snyder and Adler (19, 29), Walker (30), and Thiers (31). Ideally, in the absence of dispersion, the signal output would be a train of flat-topped peaks. Transitions from the flat part of the peak (steady-state) to the baseline would be instantaneous, and the signal from the steady-state measurement would be proportional to the analyte concentration. The actual observation, however, is that the transitions to and from the steady-state condition are skewed. These are rise and fall curves and can be seen in Figure 1-2. The experimental curve is made up of two contributing factors, the longitudinal (exponential) and axial (near-Gaussian or Poisson) contributions to dispersion. Each of these factors is discussed below.

2. Longitudinal Dispersion

Longitudinal dispersion occurs in the unsegmented zones of CFA systems. Such zones would be the sample lines (before the mixing tee), flow cell debubblers, and flow cells. In these areas, dispersion from mixing effects is dominant and the deviations from the ideal square-wave signals

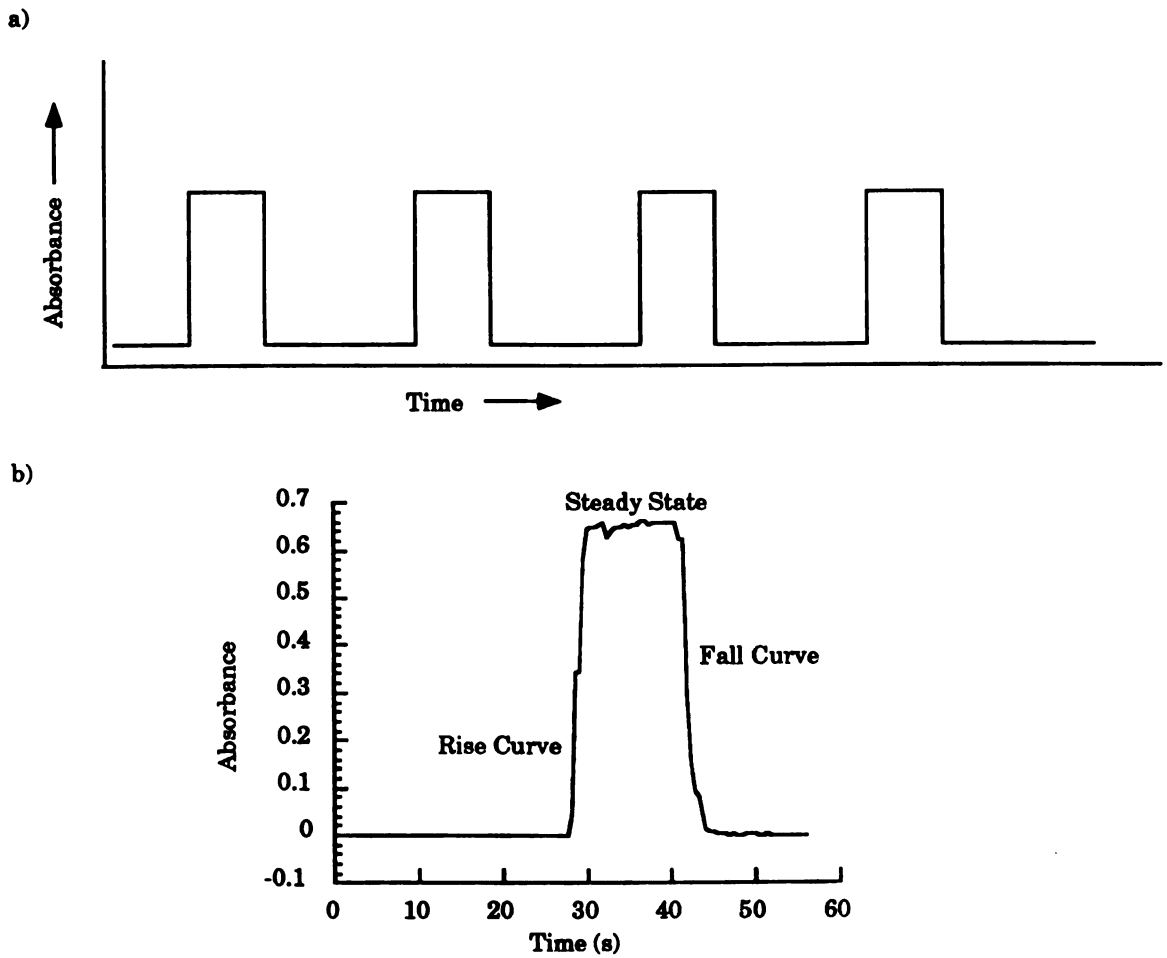

Figure 1-2. (a) The ideal, flat-topped, CFA peak. (b) The actual, experimental CFA peak.

are exponential (9). Thiers *et al.* (31) first reported a rough version of the relationship between concentration and time for longitudinal dispersion, and then Walker *et al.* (30) reported the formalized version in Equation 1.1. The theoretical linear relationship is:

$$\ln (A_{SS} - A_t) = \ln A_{SS} - t/b \qquad (1\text{-}1)$$

In this equation A_{SS}, is the steady state absorbance, A_t is the absorbance of the peak profile at time t, and b is the exponential factor or slope constant. Here, b is the time required for the detector signal to change from any value of A_t to a value of $0.37A_t$ (8). Because of the exponential relationship between absorbance and time, the sampling times to obtain peak heights within desired percent steady states can be readily predicted as values of b. For example, to obtain peak heights within 99% of the steady state, a sampling time of $4.6b$ is needed (32). Percent interaction can also be calculated as a function of sample and wash time. For example, to obtain a percent interaction of 0.5, the time between samples must be $5.3b$ (32). This model assumes that longitudinal dispersion is greater that axial dispersion.

Longitudinal dispersion can be compensated for in various ways. These ways include bubble gated flow cells (23,28,33), pecking samplers (34), or by curve regeneration (27,35). In curve regeneration, the final steady-state absorbance is calculated from Equation 1-2.

$$A_{SS} = A_t + b(dA_t/dt) \qquad (1\text{-}2)$$

Patton has shown both bubble gating and curve regeneration to be effective for reducing the effects of longitudinal dispersion (27). Curve regeneration, in particular, allows peak heights to more nearly approach steady-state and to reduce sample plug interactions. As a result, the peak profiles more closely resemble ideal peak shapes.

3. Axial Dispersion

The other important contribution to peak shape comes from axial dispersion. In CFA, mixing between segments is prohibited by air bubbles, while mixing within segments is enhanced by bolus flow (29). Thus, the the only mechanism for intersegment analyte transfer is by the stagnant liquid film left on the walls of the flow system after each successive sample and wash. The concentration of analyte molecules in any segment is approximated by Equation 1-3 (36).

$$C_k/C_0 = e^{-q}\, q^k/k! \qquad (1\text{-}3)$$

where C_k is the analyte concentration in segment k (k=integer), C_0 is the concentration of the initial sample (k=0), and q is a dimensionless parameter which is the ratio of the volume of liquid that wets the walls of the entire flow system (V_f) to the volume of a single liquid segment (V_s). When considering a CFA system, the sample is a series of analyte-containing segments, so the concentration distribution is represented by the summation of Equation 1-3. For a large number of segments, the initial Poisson distribution evident by the right-hand side of Equation 1-3 closely approximates a Gaussian distribution. Thus, axial dispersion is conveniently expressed as the standard deviation, σ_t , of the Gaussian

curve. Equation 1-3 was the initial attempt to model axial dispersion, and unfortunately, fails to relate axial dispersion to experimental variables such as residence time, flow rate, segmentation frequency, and inner tube diameter.

4. Snyders Equation

In 1976, Snyder and Adler developed an extensive model of axial dispersion that expresses q in terms of experimental variables and thus allows σ_t to be related to these variables (19). The derivation also allows V_f to be expressed in terms of the length and diameter of the flow system. Snyder and Adler (36-39) also extended previous models by accounting for previously unaccounted for slow mixing between segments and liquid film (29). In 1976, Snyder expressed his axial dispersion equation in a form that shows the effects of major experimental variables (20). The model makes the following several assumptions (20):

1. Air segment volumes are the minimum required to totally occlude a tube of a given inside diameter ($(7/24)\pi d_t^3 = 0.92 d_t^3$).
2. The CFA system is perfectly wetted.
3. Longitudinal mixing within the film is negligible.
4. The flow system is free from longitudinal dispersion (i.e. mixing effects).

Snyders' equation is shown in Equation 1-4.

$$\sigma_t^2 = \left[\frac{538 d_t^{2/3}(F + 0.92 d_t^3 n)^{5/3}\eta^{7/3}}{\gamma^{2/3} F D_{w,25}} + 1/n\right]\left[\frac{2.35 (F + 0.92 d_t^3 n)^{5/3}\eta^{2/3} t}{\gamma^{2/3} F d_t^{4/3}}\right] \quad (1\text{-}4)$$

where:

σ_t = the standard deviation of the peak (s)
d_t = the internal diameter of the flow system (cm)
F = the liquid flow rate (mL/s)
n = the segmentation frequency (Hz)
t = the residence time of the sample in the flow system (s)
η = the viscosity of the liquid (poise)
γ = the surface tension of the liquid (dyn/cm)
$D_{w,25}$ = an empirical diffusion coefficient that pertains only to diffusion in coiled tubes (cm^2/s) (20)

The assumption that the flow system is perfectly wetted in insured by adding a surfactant, such as Brij 35, to the flowing stream. It is also obvious that the standard deviation of the peak varies directly with the square root of time, and, as a consequence, sample residence time should be kept to the minimum time necessary for the reaction to go to completion. The effect of flow rate, internal diameter of the flow system, and segmentation frequency can be visualized by plotting the standard deviation as a function of segmentation frequency for different values of flow rate and internal diameter, while time is held constant. An example of such a plot is given in Figure 1-3, and many other examples of such plots are easily found (20,21,40). The important conclusions to draw from these plots is that for any flow rate, optimum values of inner diameter and segmentation frequency exist where the dispersion is a minimum, and, because the minima are relatively flat, variations in flow rate or segmentation frequency, by as large as a factor of 4, only affects the dispersion by about 5% (20). It should be noted that, from Figure 1-3b, it appears that by simply decreasing the flow rate, even lower dispersion values could be obtained. However, to do this, the inner diameter must be decreased, and the

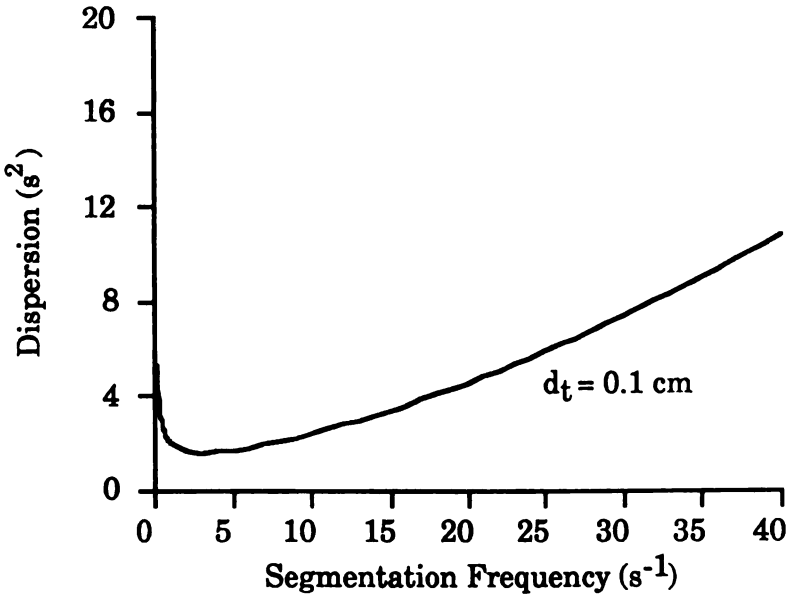

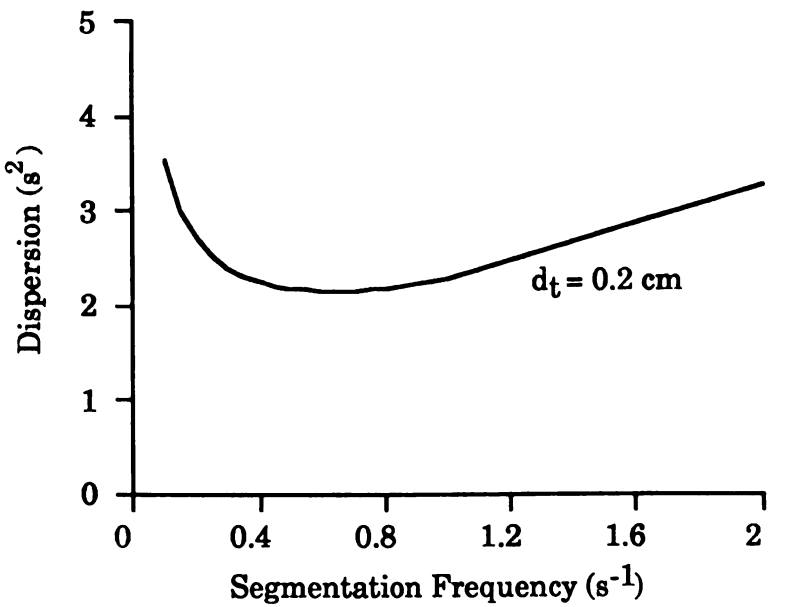

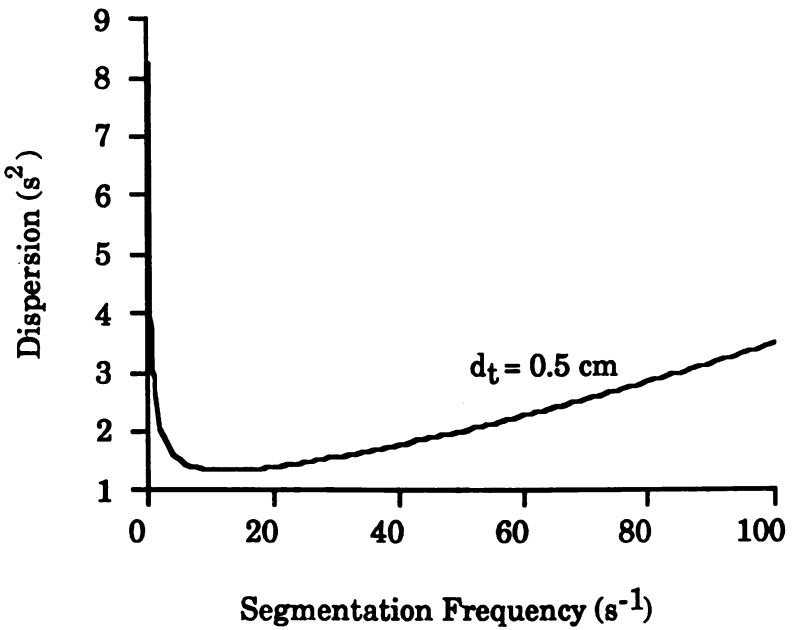

Figure 1-3a. The effects of segmentation frequency, flow rate, and internal diameter of the flow system on dispersion. F=0.0083 mL/sec, other variables are as in Ref. 27.

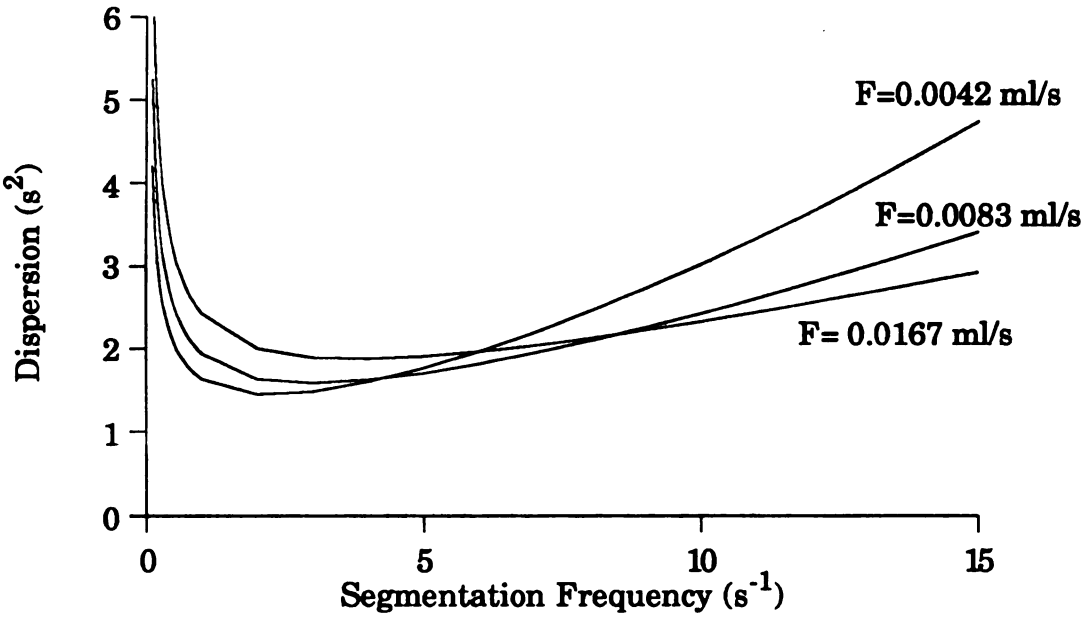

Figure 1-3b. The effects of segmentation frequency, flow rate, and internal diameter of the flow system on dispersion. For this plot, d_t = 0.1 cm. All other variables are as found in Ref. 27.

segmentation frequency increased. Thus, practical constraints such as back pressure, flow-cell volumes, and clogging will most likely limit new efforts to reduce dispersion in these systems (41).

D. Comparable Flow Reversal and Flow Recycle Systems

1. Introduction

As the research in this thesis pertains to flow reversal and flow recycle continuous flow systems, it is necessary to review the current state of affairs in Flow Reversal techniques (42-53). Currently, the major emphasis on flow reversal techniques has been when coupled with Flow Injection Analysis (FIA). For example, Betteridge and Wade have been employing flow reversal flow injection techniques to manipulate concentration gradients for either equilibrium-based speciation or optimization studies (44,47,49). Toei has developed a method for the determination of glucose in clinical samples by flow reversal FIA (51-53), while Valcarcel and coworkers have been undertaking the study of multidetection with a single detector (42, 43, 45, 46, 48, 50).

2. Flow Injection Analysis

To be able to talk about these flow reversal FIA systems, a short introduction to the principles of FIA is in order. In Figure 1-4a, a typical CFA set-up is shown and compared to the usual FIA system (Figure 1-4b). The average FIA system consists of an injection valve, a reaction manifold, and a detector. In the FIA system, a nonsegmented carrier stream is pumped continuously through a reaction manifold and then through a detector. Samples are introduced into the carrier stream (typically) through the use of a six-port valve. This six-port valve has a sample loop,

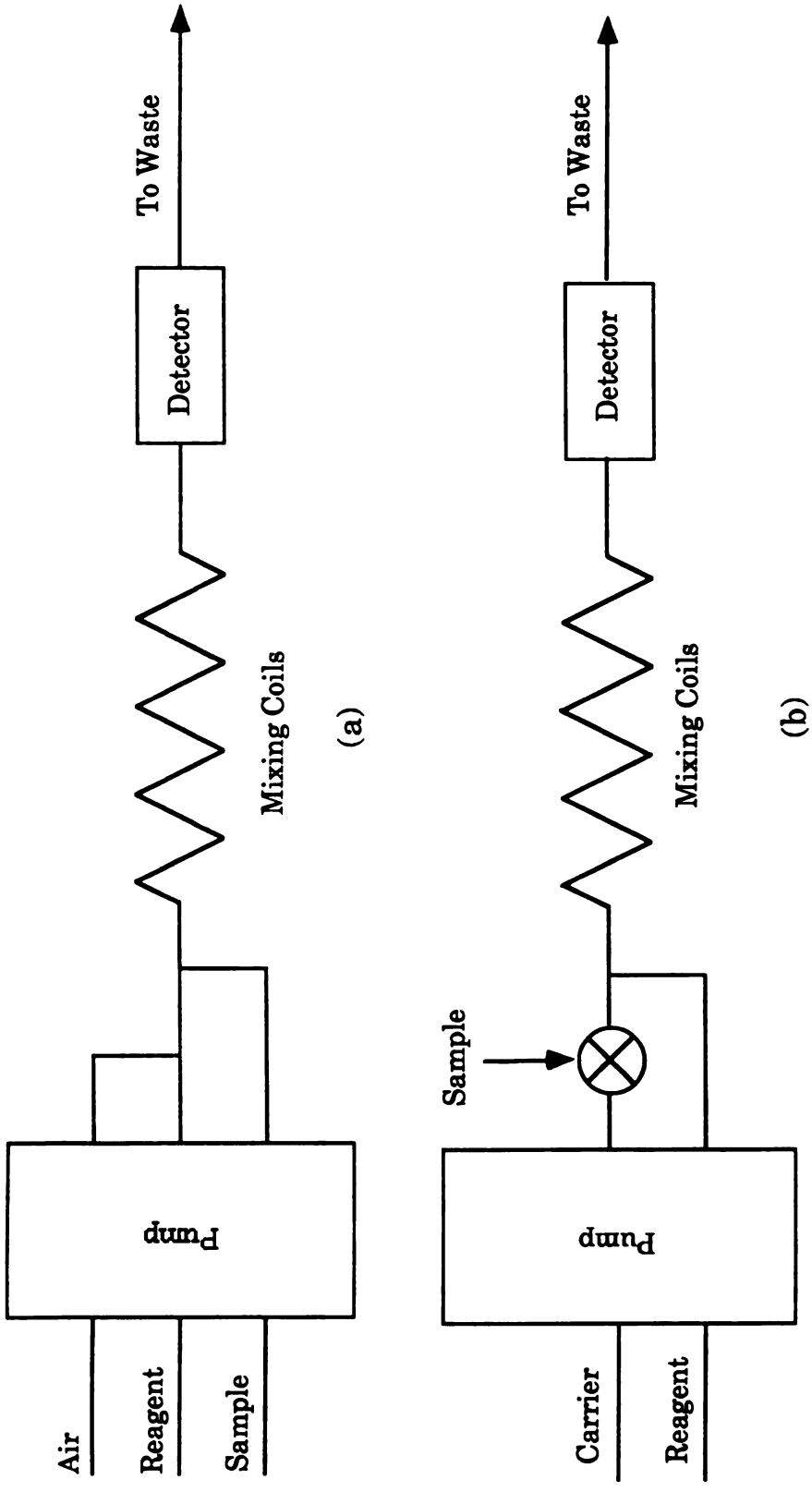

Figure 1-4. (a) A typical CFA set up with Air, Reagent, and Sample. (b) A typical FIA set up where the sample is merged in the reagent stream in a nonreactive carrier stream.

which determines the amount of sample introduced into the system. After injection, the sample and the carrier stream are mixed and sent to the detector. Thus, the sample, at injection, is a well defined sample plug, but, as it travels towards the detector, the sample mixes with the carrier stream and dispersion occurs. This results in peak shapes for FIA typically being skewed Gaussian, as opposed to CFA peaks having flat tops. The dispersion in the FIA system is due to the internal geometry of the tubing, the flow profile, and the molecular dispersion (8).

3. FIA Systems for Concentration Gradients

Betteridge and Wade have initially studied several flow reversal-type configurations (44,47,49). These studies involved the use of one or more pumps, only one detector and one or more valves. One configuration involved a system that performed a single reversal without a reaction; they found that the heights of the peaks as a a function of time dropped in an exponential manner. This is explained by the fact that, in their configuration, the plug had to travel further backward than forward to reach the detector. A second configuration involved multiple reversals without a reaction, with this configuration differing from the first by adding a valve and removing a pump. The resultant peaks were tending toward Gaussian, with the peak heights slowly decreasing. Finally, a single reversal with reaction was performed to demonstrate the applicability of such a system. The proposed system (49) was to be used to manipulate concentration gradients for equilibrium-based speciation or optimization studies.

4. Multidetection Systems

Toei developed a flow reversal FIA system for the determination of glucose in clinical samples (51-53). His system is a multidetection, open flow stream configuration and involves the use of only 1 pump and 1 detector. This makes his apparatus relatively simple. In this configuration, samples are passed through a detector and then pumped back to the same detector in the reverse direction by use of the same pump. The flow direction is reversed by employing the use of a six-port valve. In this configuration, at least two pieces of information were obtained from each sample. The amount of dispersion was not found to be significantly greater than in the typical FIA system. The effect of several experimental parameters, such as the effect of flow changeover time, the mechanical stability of the system, the effect of reaction time, reaction temperature, sample volume, reagent volume, and the flow-rate of carrier stream were studied. One problem encountered was increased baseline noise during the flow changeover due to the rotation noise of the valve, but this noise was deemed inconsequential because it did not affect the actual analysis. Toei also found that peak areas were very reproducible, and as such, should be suitable for kinetic determinations of analytes using two-point assays.

5. General Flow Reversal Techniques

The group of Valcarcel and coworkers in Spain has been very active in the investigation of flow reversal FIA techniques. Their emphasis has been on using flow reversal techniques for multidetection in kinetic-based determinations. They have previously investigated the possibility of obtaining dual peaks by injecting unusually large sample volumes (54), by splitting the sample plug and then recombining the streams prior to

detection (55), or by using two injection valves located in series, parallel, or coupled internally (56-58). The more recent work of Valcarcel *et al.* has been in studying multidetection in open systems (42,45), and these are the systems that are more applicable to the flow reversal/flow recycle CFA systems described in this thesis.

The initial flow reversal FIA system was first described in 1985 (42) and was designed using principles first demonstrated by Jensen *et al.* (59,60) and Hooley and Dessy (61). This system involved the use of one detector, one pump, and one switching valve. A second valve was added to perform sample injections as necessary. The configuration was evaluated by using three systems. One was without a chemical reaction, one monitored the disappearance of a product, and one monitored the appearance of a product. The influence of typical FIA variables (flow rate, reactor length, etc.) as well as the influence of chemical variables (pertinent to the chemical system being studied) were determined.

Several other applications of this configuration or simple variations of it have been demonstrated. In one instance, they used a flow reversal FIA system to determine the viscosity of water-miscible samples (48). In other cases, they used this system to perform individual and simultaneous determinations (42,45), to do speciation studies (62), and to calculate the reaction stoichiometries (46).

Chapter 2

Instrumentation, Software, and Data Processing Techniques

A. Overview

In this chapter, the design of the CFA system is described. Particular attention was given to the physical descriptions of the various (4-port and 6-port) valve configurations, with special emphasis placed on the 6-port configurations. Also included is a brief description of the individual parts of the CFA system, as well as manifold design considerations. (For more detailed information of individual design and construction, consult the Ph.D. dissertation of Patton (27)). Finally, a discussion of the computer techniques written for the system is presented.

B. Set-up

A general diagram of a reversal/recycle apparatus is shown in Figure 2-1. It consists of a pump, a manifold, two switching valves (one four port and one six port), a source, a double beam detector (colorimeter), some type of debubbling system (either physical or electronic), and power supply. Components are described in detail later in this chapter.

The system is operated in a typical CFA manner. The sample, buffer and reagent(s) are introduced into the system through immersion of the pump tubes into vials of solution and pumped into the manifold. Once in the manifold, the sample, buffer, reagent(s), and air are mixed and sent through mixing coils. After a period of time in mixing coil 1 (the time is

determined by the length of the coil and the flow rate), the sample is pumped through the colorimeter and now, unlike typical CFA systems, is pumped into a holding coil 2 (see Figure 2-1). Once all the sample is pumped through valve B and into the holding coil, the flow is reversed by switching valve A and is thus sent back through the colorimeter for another measurement. This reversal procedure is continued until the desired number of measurements are obtained or the indicated number of reversals are accomplished.

In the recycle configuration (see Figure 2-2), valve B is switched after the last sample has gone through. Now the stream is being propelled by the buffer coming through valve B. Valve A is switched immediately after the switch of valve B, and thus the sample flows through valve A and into coil 1. Once all the sample is completely in coil 1, both valves are switched again. The sample is now propelled by the buffer stream entering through valve A and proceeds through the colorimeter again. The whole process then repeats itself as many times as indicated by the user.

The complete arrangement of equipment for the flow reversal/flow recycle apparatus is shown in Figure 2-3. Helium gas is used to turn the valves quickly, and an Opto-22 is used to convert and then relay the TTL signal from the RTI data acquisition board to the solenoid/actuator. Descriptions of all other components are given in this chapter. Detailed valve configurations are shown for flow reversal in Figures 2-4 and 2-5, while valve configurations for flow recycle are shown in Figures 2-6 and 2-7. Configurations are given for both valve A being a 4 port and a 6 port valve, with valve B always a 6 port valve. Currently, the system is operated on the two 6 port configurations.

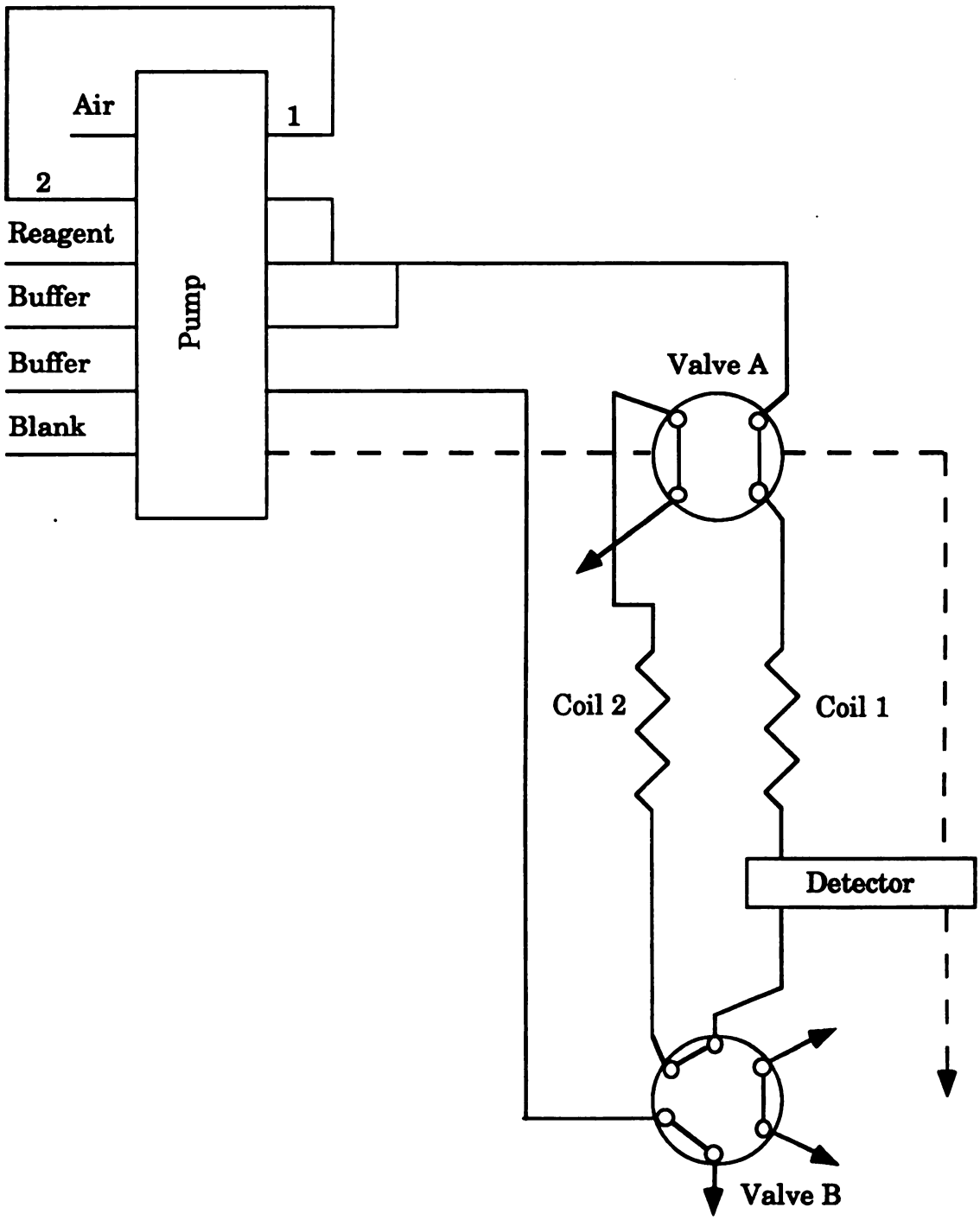

Figure 2-1. The general schematic for the Flow Reversal Continuous Flow system.

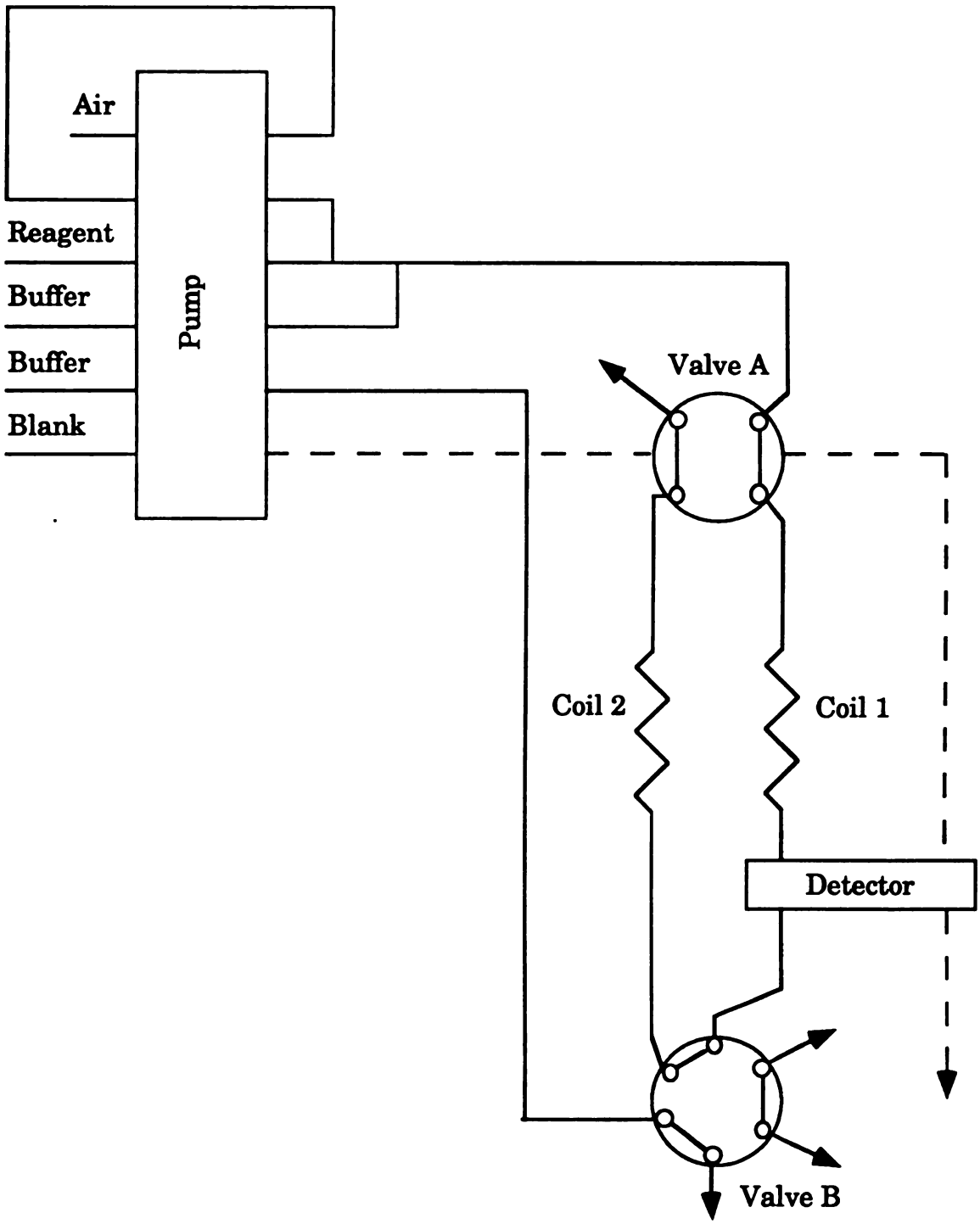

Figure 2-2. The general schematic of the Flow Recycle Continuous Flow system.

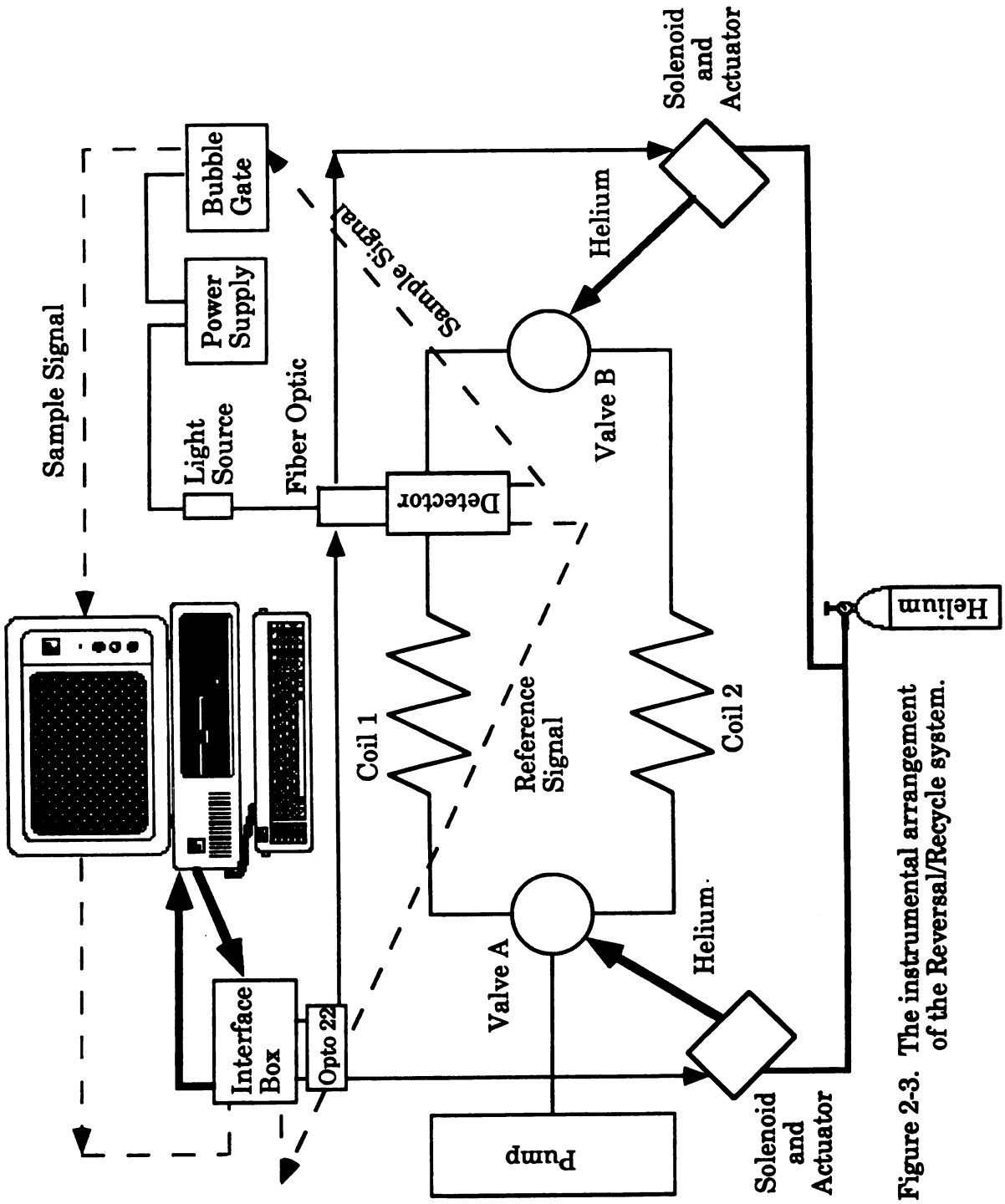

Figure 2-3. The instrumental arrangement of the Reversal/Recycle system.

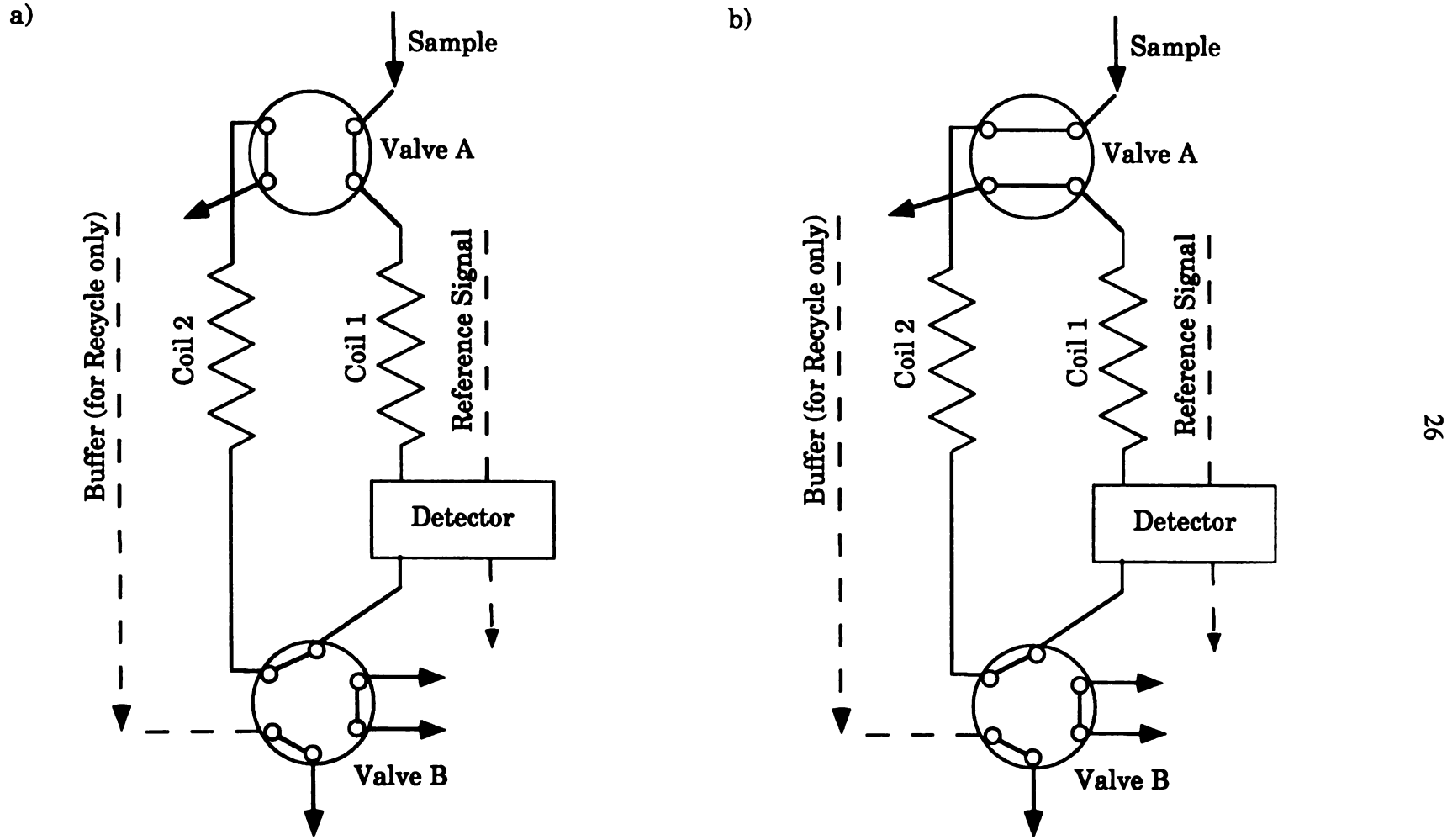

Figure 2-4. The valve configuration for flow reversal CFA with a 4-port and a 6-port valve. a) shows the initial position while b) shows the valve configuration after a reversal. Notice that in the reversal configuration, valve B is stationary. Note: All arrows exiting valves go to waste.

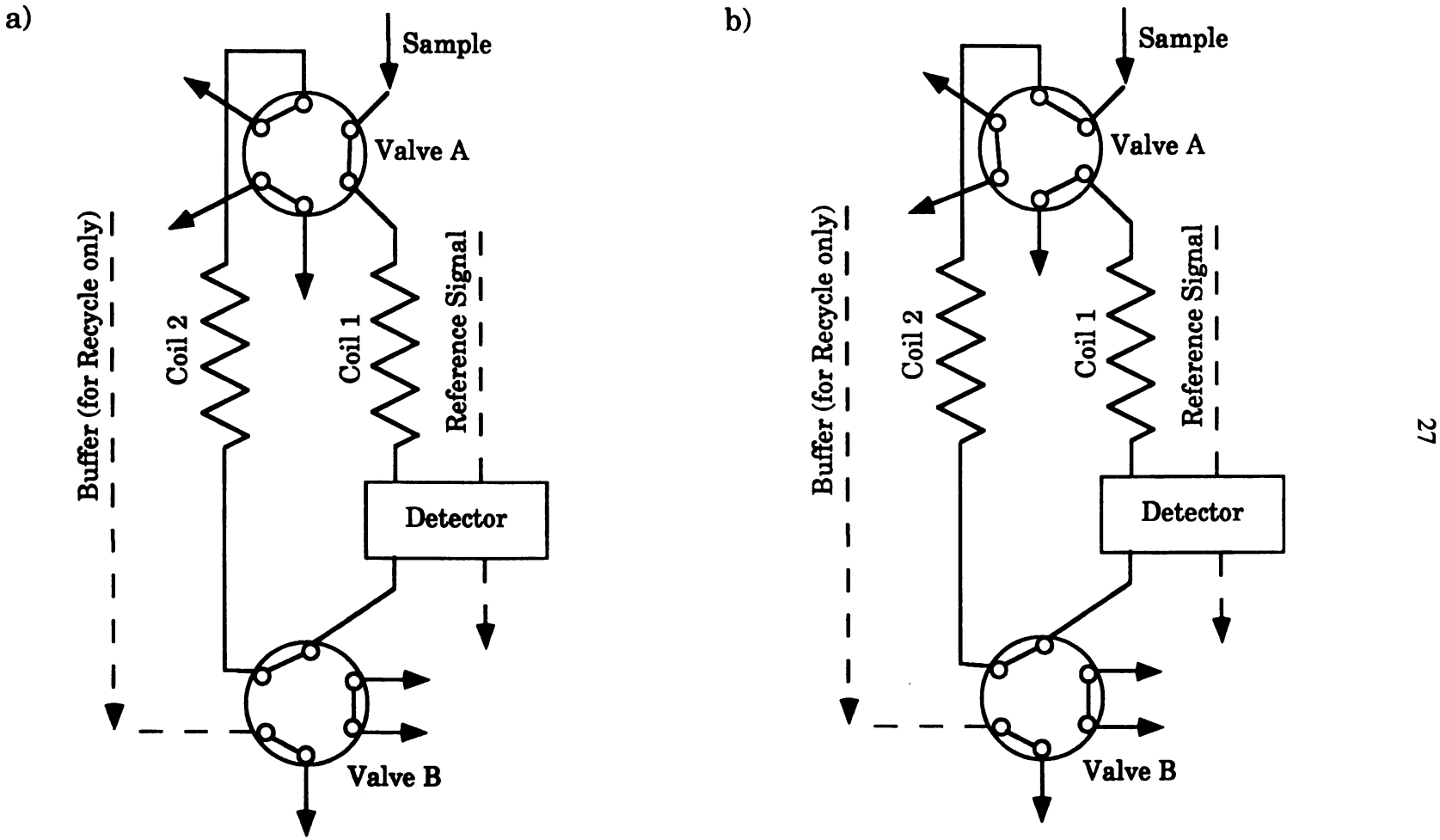

Figure 2-5. The valve configuration for flow reversal CFA with two six port valves. a) shows the initial position while b) shows the valve configuration after a reversal. Notice in the reversal configuration, valve B is stationary. Note: All arrows exiting valves go to waste.

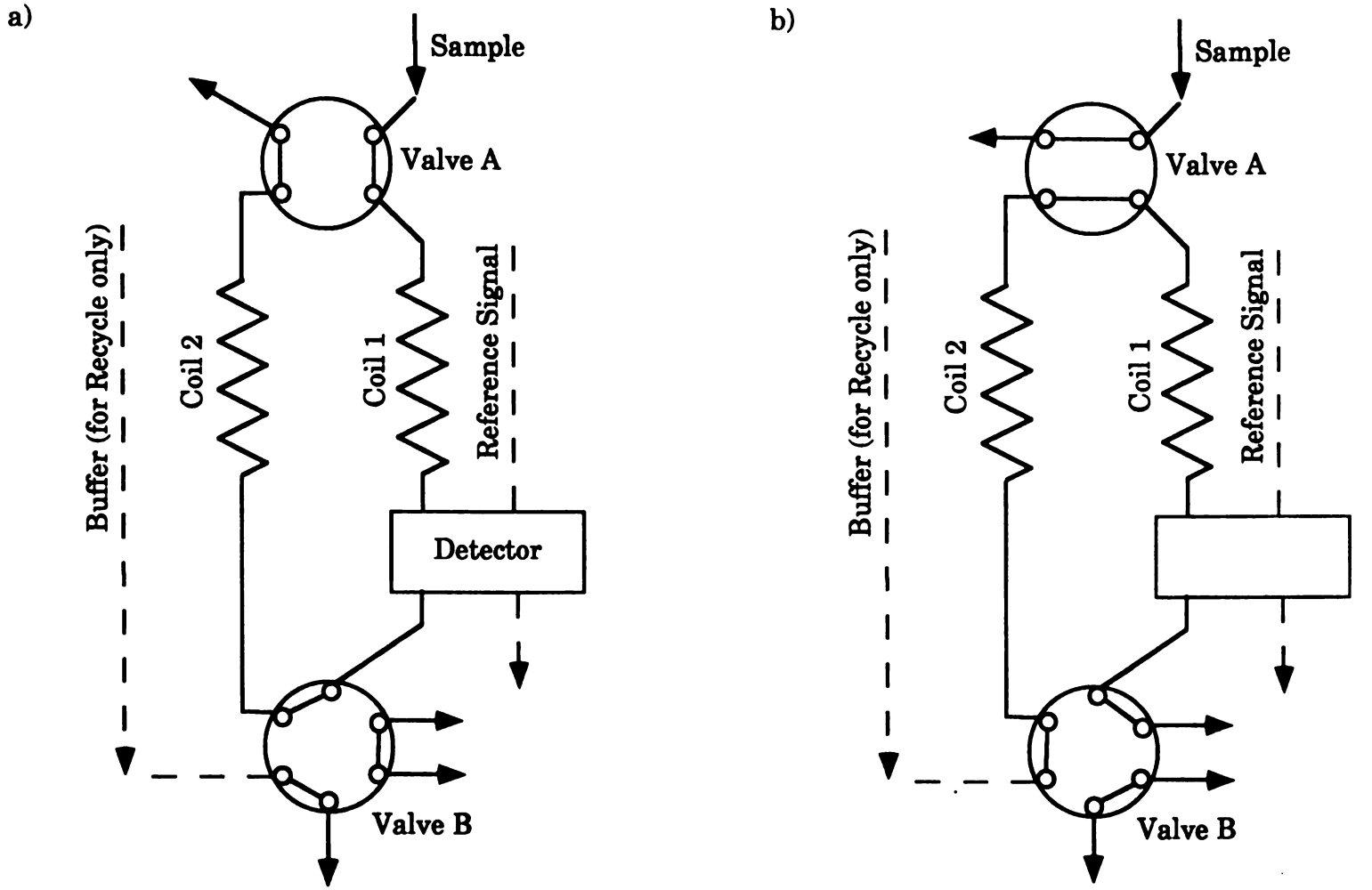

Figure 2-6. The valve configuration for flow recycle CFA with a 4-port and a 6-port valve. a) shows the initial position while b) shows the valve configuration after a recycle. Notice that in the recycle configuration, both valves are turned. Note: All arrows exiting valves go to waste.

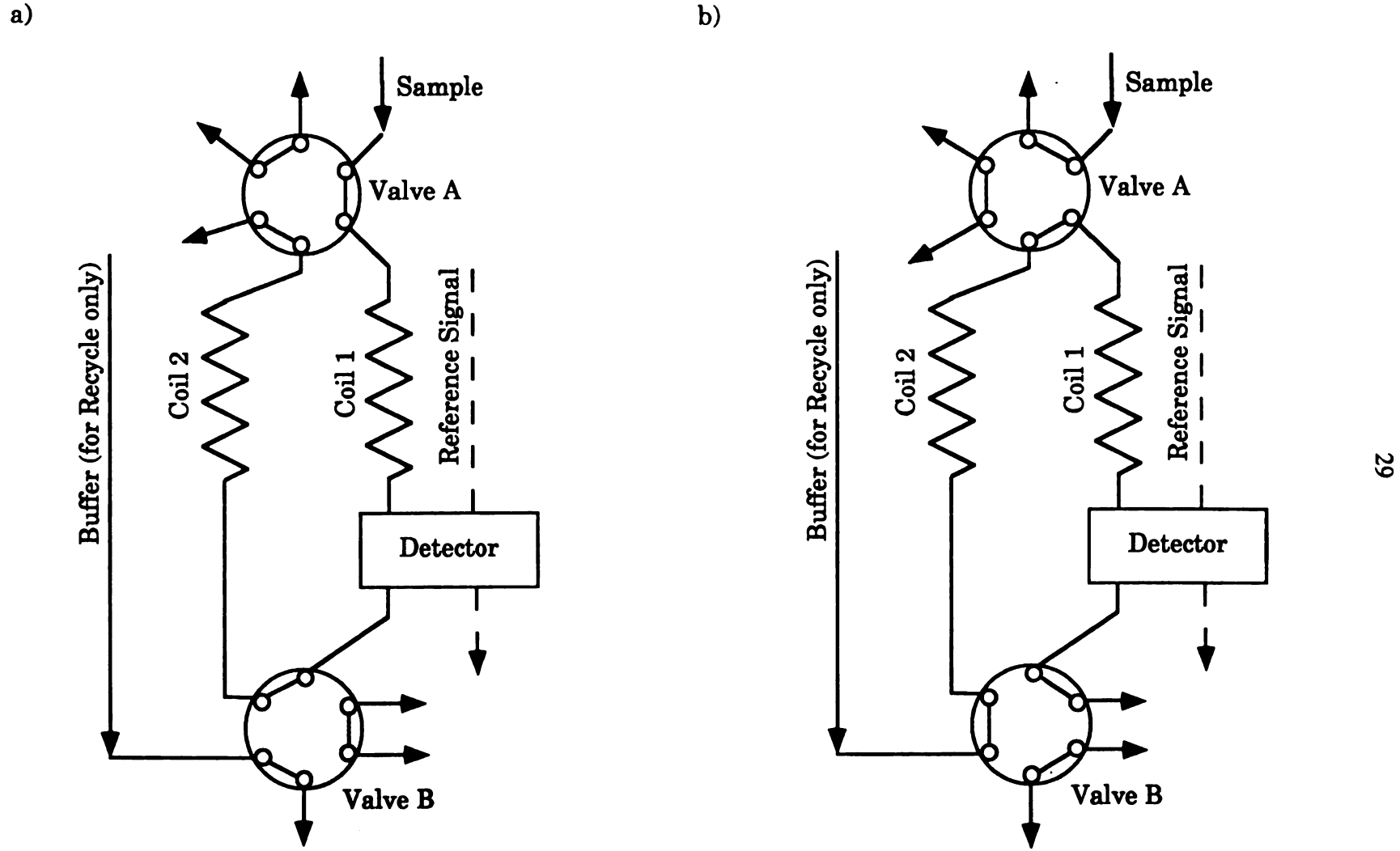

Figure 2-7. The valve configuration for flow recycle CFA with two six port valves. a) shows the initial position while b) shows the valve configurations after a recycle. Notice that in the recycle configuration, both valves turn. Note: All arrows exiting valves go to waste.

C. Components

1. Pump

The pump used in all experiments was the Model IP-12 variable speed, 12 channel peristaltic pump from Brinkmann Instruments (Westbury, NY). It was modified in-house by replacing the standard 8 roller assembly with a 16 roller assembly (27). The pump motor speed is controlled by a two decade digital control that provides for linear motor speed adjustment, as shown in Figure 2-7. The two decade controller has a range of values from 00-99. A nominal pump setting of 44 was needed for experimental flow ratings to agree with rated flow values for Technicon SMA Flow-Rated pump tubes.

Technicon SMA Flow-Rated pump tubes were used in all the experiments. Flow rates for the pump tubes at various pump settings are easily calculated through a delivery factor determined for the individual pump and the flow rating of the pump tubing. It is typical to operate at the nominal pump speed and change tubing diameter, rather than change the pump setting. A table giving the flow rate of various tubings at the nominal flow rate can be found in Table 2-1. Each piece of flow tubing has plastic shoulder markers at each end indicating tube identity, corresponding to a certain flow rate. Lubricant is applied regularly to extend the flow tube life.

Table 2-1. Flow rates for various pump tubes at the nominal pump speed setting of 44.

Color Code of Pump Tubing	Nominal Flow Rate (mL min^{-1})
orange-black	0.015
orange-red	0.030
orange-blue	0.050
orange-green	0.100
orange-yellow	0.160
orange-white	0.230
black-black	0.320
orange-orange	0.420
white-white	0.600
red-red	0.800
grey-grey	1.000
yellow-yellow	1.200
blue-blue	1.600
green-green	2.000

2. Addition of the Air Bubble

There are two methods that can been used to add air segments to the flowing stream (27,63). The first method was developed by Habig *et al.* (63), and is shown in Figure 2-1. It uses two pump tubes (1 and 2) connected in such a manner that tube 1 acts as a compressor for tube 2. Tube 2 is then connected to the air inlet of the manifold. Thus, identical segments of compressed air are trapped between the pump rollers and when the forward roller leaves the pump platen, the air rapidly expands into the manifold and creates the air bubble.

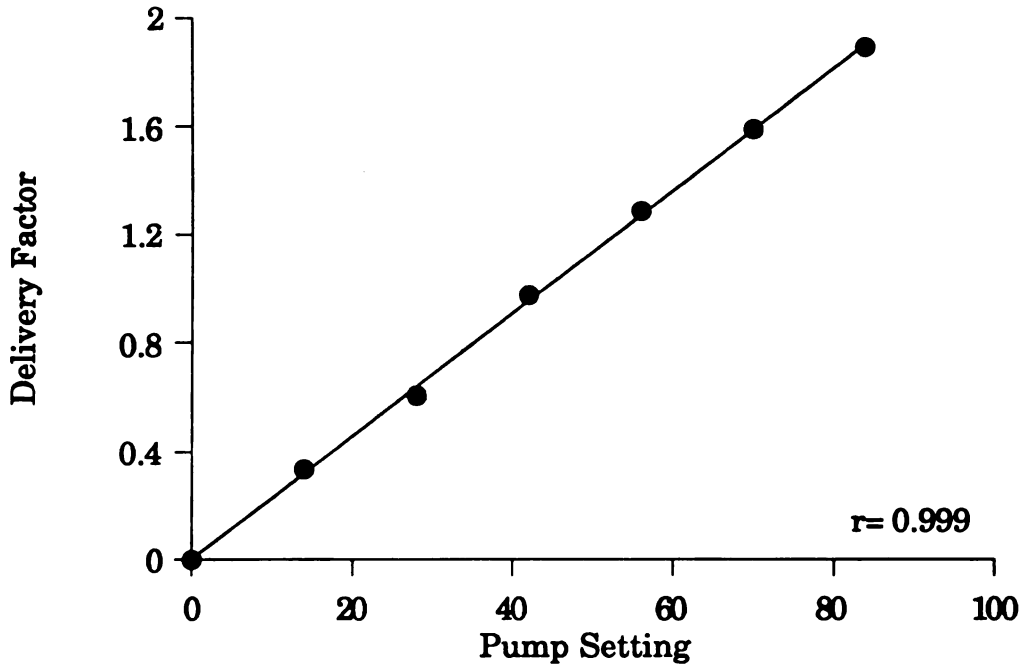

Figure 2-8. A plot of pump tube delivery factor versus pump setting, indicating that linear pump motor speed adjustment is possible. The delivery factor is the value by which the nominal pump tube flow rate must be multiplied to estimate actual flow rate.

The second method was developed by Patton (27). It involves the use of an optical chopper, which used information from an opto-interrupter to add gas from a low pressure gas tank in sequence with the movement of the pump rollers. This method of phasing used a solenoid valve and the connection between the gas tank and the manifold. Advantages to this method include a reduction in the number of required pump channels and air segments can be added in phase with every second, third, or a forth, roller lift-off.

In this work, air segments are added using the first method. This is because the method is simple and has been proven reliable, and optimal flow rates for tubes 1 and 2 had already been determined to be 0.05 and 0.1 mL/min (27).

3. Colorimeter

A double beam, fiber optic photometer was designed, built and characterized for the miniature CFA system by Patton and a detailed description has been given (27). A block diagram of the photometer is shown for reference in Figure 2-8.

The light source for the detector is a miniature tungsten-halogen lamp. The source is then connected to the front windows of the flow cells by a fiber optic. This connection is accomplished through the use of rectangular, black Delrin© blocks that slide along grooves in the base of the photometer. The flow cells have a pathlength of 1.0 cm, an internal diameter of 0.05 cm, and are made with sapphire windows. Three-cavity interference filters are used to permit wavelength discrimination. These filters are 1.27 cm in diameter and have approximately an 8 nm bandwidth. Easy removal, installation, and proper optical alignment is assured through holes drilled to a depth of 0.2 cm in the face plate.

The detector circuitry is encased in a metal cover. The inside circuitry consists of two silicon photodiodes to detect the radiation and to convert the radiant power to photocurrent. Current-to-voltage conversion is accomplished through the use of operational amplifiers. Variable gain amplifiers are used to amplify the output from the current-to-voltage converters. Channel 1 and channel 2 signals are connected to the inputs of

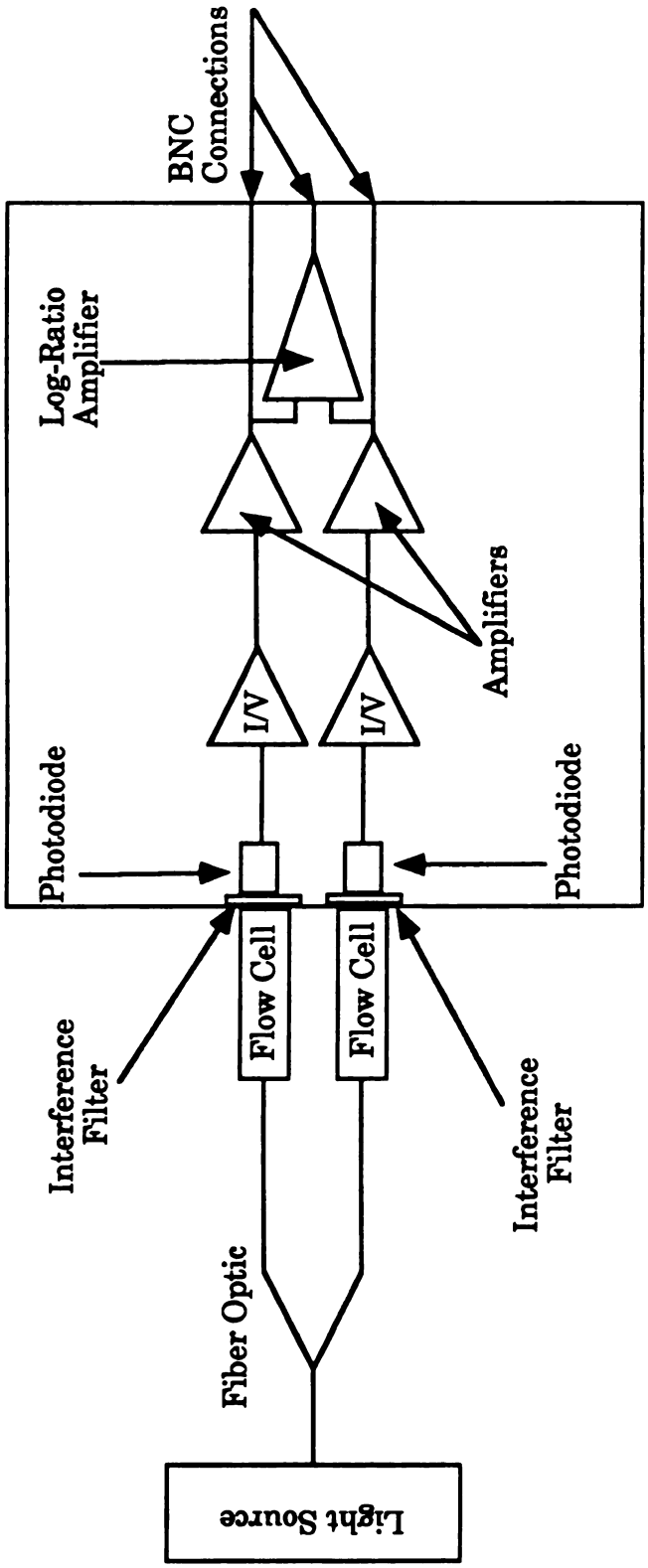

Figure 2-9. A schematic diagram of the double-beam, filter photometer used in this CFA system.

a log-ratio amplifier for direct readout of absorbance. Signal outputs are made available through BNC connectors mounted on the back of the detector housing.

4. Bubble Gate

An electronic bubble gate is used to remove the unwanted portion of the signal that is caused by the passage of the air segment through the detector. It has been described both electronically and physically by Patton *et al.* (28). This bubble gate uses the fluctuations in the detector signal that are caused by the change in refractive index as the air and liquid segments pass through the detector to synchronize the time of data acquisition to include only those times that the liquid segment completely fills the flow cell.

5. Manifold Components

Manifold components such as tee's, mixing, coils, connectors, etc., were constructed locally. Some pieces had been made previously, while new parts were fabricated using expert advice (9, 27, 64). All the mixing tees and four inlet mixing components were made previously (27), and allow for zero dead volume connections between sample, air, and reagent tubes and the manifold. However, new mixing and sample coils were made recently.

The mixing coils were made out of polyethylene tubing. The procedure used was similar to the process pioneered by Amador (64). Various lengths of polyethylene tubing were wrapped around 3.0 cm glass lengths and their ends taped off by masking tape. The rod/tubing combination was placed in boiling water for approximately 5 minutes and

then placed in cold water for 1 minute. After the final minute, the combination was allowed to dry and then the resultant coil removed from around the glass rod. These coils have a number of advantages when compared to glass mixing coils. These advantages include cost, durability, ease of construction, flexibility, and compatibility with fittings that allow for zero dead volume connections to be made between the coils and tees. The disadvantage of these coils is that they are less wettable than glass coils, which results in bubble-break-up due to back pressure created in the CFA system. However, this problem can be overcome through the use of a surfactant such as Brij-35.

6. Valves

The valves used in this work are 6-port valves mounted on pneumatic actuators. The actuators are connected to solenoids, which use helium gas to turn the valves. Helium, as opposed to compressed air or argon, is used because the valves need to be turned quickly and helium was determined to switch valves the quickest.

7. Other Connections

Some connections between tubes cannot be made directly. For example, short pieces of Teflon tubing were inserted into the ends of the pump tubing for use as sample, reagent, and buffer withdrawal lines. The pump tubing was not always of small enough diameter to provide for a secure fit, so plastic sleeves were used to better the fit between the outer diameter of the Teflon tube (typically 0.05 cm) and the inner diameter of the pump tube. Also, connections between the manifold fittings and the

delivery ends of the pump tubing were improved in this manner, as needed. Worn pump tubes were saved for just such purposes.

D. Sample Introduction

In CFA, samples pass through the pump before they reach the manifold. In this time period before reaching the manifold (and the point of insertion for the air bubble), the sample undergoes mixing and dispersion (because of the laminar flow conditions) between either successive samples or between sample and wash solution. The intersample air segment (IAS) that is introduced into the line when the line is switched between sample and wash serves as a small barrier to intersample mixing. Further reduction of the intersample mixing and dispersion can occur if the sample line is "pecked". Pecking involves the quick removal and insertion of the sample line three or four times when exiting the sample solution and entering the wash solution and vice versa. Patton has shown this to be extremely effective for lowering the mixing within a sample (27).

E. Data Acquisition and Processing

Data were acquired through the use of an IBM PC (8088) computer. A program was written to control the Continuous Flow Reversal/Recycle apparatus, using the initial parts of a data acquisition routine written earlier in this laboratory (65,66). The program is called DBEAM. It was written in a "user friendly" format, which prompts the user to enter all the necessary parameters for an experiment. It also allows for the correction of incorrectly entered parameter information. A block diagram showing the "logical thought progression" of the routine is shown in Figure 2-9.

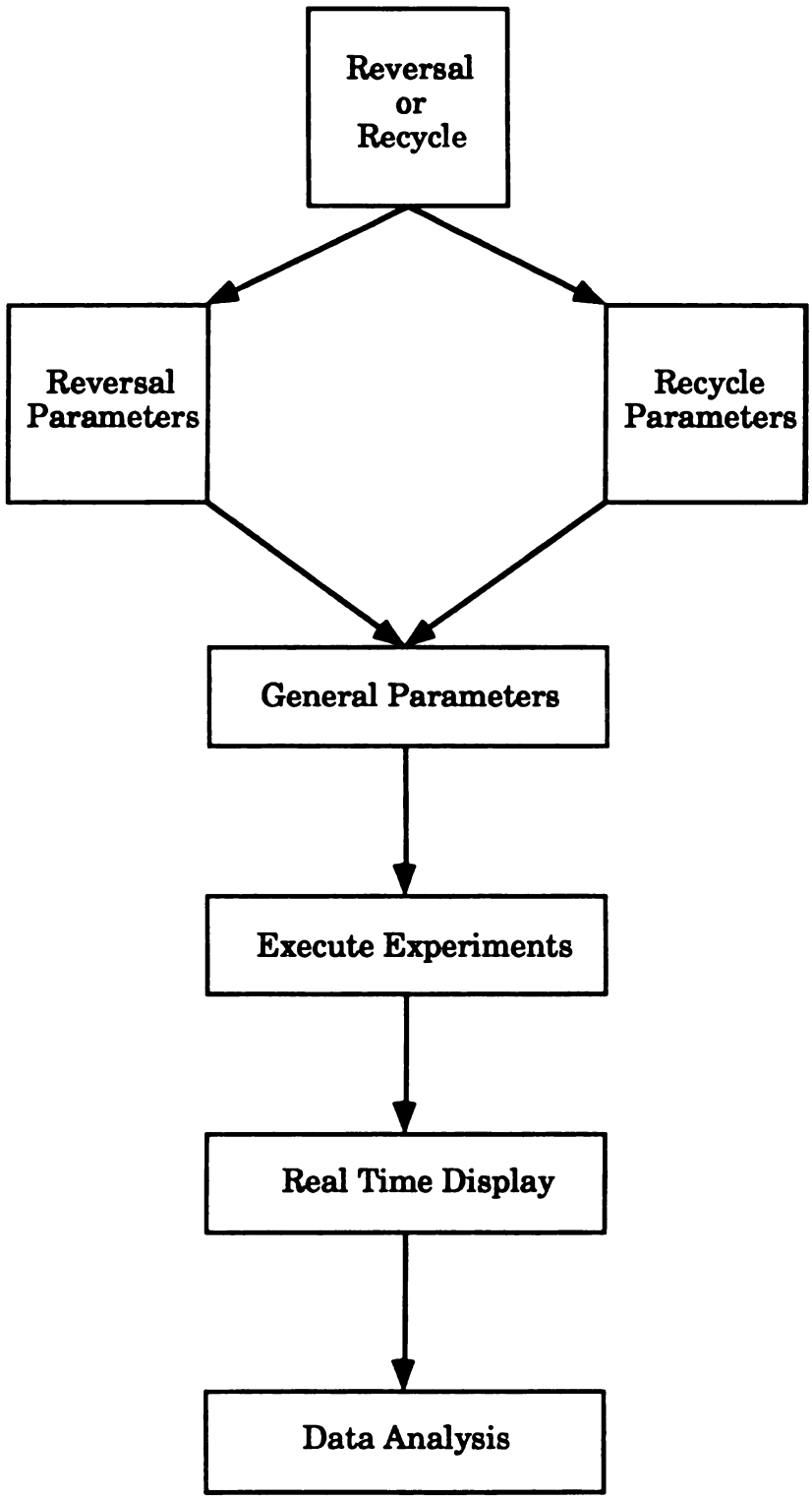

Figure 2-10. The "thought process" of the CFA Flow Reversal/Recycle program.

The initial choice presented to the user is "Reversal or Recycle"? Based on the users response, the user is taken through a series of screens that are aimed at obtaining the parameters necessary for the experiment. The reversal or recycle parameters ask the user for parameters that are specific to the technique, while the general parameters obtain parameters that would be the same for either experiment. After all the variables are approved by the user, the experiment is started on the indication of the user. A real time display presents information to the user that is indicative of the experiment. After all the data have been collected, the user is given the option of examining the data in graphical form.

1. Specific Experimental Parameters

In the flow reversal configuration, there are only a few parameters needed to be known that are specific to this experiment. They are 1) number of samples 2) number of reversals and 3) the desired threshold (parameter used to determine whether a peak has passed through the detector, and discussed in greater detail later in this chapter). From this information, the total number of peaks expected to pass through the detector is calculated so that the software can end the experiment after all the necessary information has been obtained. These values are summarized and are correctable before the user actually begins the experiment.

In the flow recycle configuration, there are a few more variables that have to be entered. They are as follows:

1. Number of recycles
2. Number of samples
3. Inner Diameter of mixing coils
4. Length of mixing coils
5. Number of inputs into the manifold
6. The flow rate of the pump tubing
7. Threshold

Again, the number of peaks expected through the detector is calculated. Also calculated is the length of time it will take for the sample(s) to go through mixing coil 2, completely through valve A, and into mixing coil 1. After all the sample is in mixing coil 1, then valve A can be switched. The expression used for calculating this time is shown in Equation 2-1.

$$\text{Recycle Delay Time} = ((100 \times \text{CoilLength})/((\text{FlowRate} \times 3.1415) \times \text{ID}^2)) \quad (2\text{-}1)$$

As usual, all these variables are user correctable before the experiment is initiated.

2. General Parameters

The general parameters give the user a chance to set variables that would be common to either experiment. These might include a delay time before data acquisition begins, solution pH, ionic strength, length of

experiment, or the detector channel information, i.e. two sample channels, one sample, one reference, single beam, etc., among others. This screen also allows the user to determine the rate of data acquisition.

3. Execute Experiment

This is simply one screen that allows the user to initiate the experiment. Data collection begins either immediately or after some user entered, preset time delay period.

4. Real Time Display

The real time display is a chart that presents the current status for all the important experimental information. Aspects such as the sample and reference voltage and the number of reversals or recycles left in this experiment are updated after the acquisition of each point. A sample screen is shown in Figure 2-10. Also note that their is a line at the end of the chart that tells the user the current status. Lines that appear here include:

1. Waiting for the start of peak # X.
2. Determined the start of peak # X.
3. In the delay period before valve switch...
4. Finishing the baseline to point # Y...

5. Data Analysis

At the current time, the software can generate a number of plots. The one used most frequently is the absorbance versus time plot, which

allows the user to immediately view his data after the run is complete. Unfortunately, the software, at this time cannot adequately calculate the area under a selected region of the curve, or give the peak maximum of a selected peak from a series of peaks. It can however, give the peak maximum for each peak. Also at this time, the user is asked if he/she wishes to save the data to floppy diskette. If the response is yes, files are written to the floppy diskette that include both the data points and relevant run information and parameters. These data files can be imported into other statistical packages for numerical analysis.

DOUBLE BEAM FLOW REVERSAL, FLOW RECYCLE CONTROL PROGRAM
DATA COLLECTION IS BEGINNING, PLEASE STAND BY

Method		Reversal
Number of Samples		3
Number of Reversals/Recycles	2	
Analyte Signal (V)		3.00
Background Signal (V)		5.00
Number of Points collected		123
Number of Points expected		451
Number of Peaks to find (overall)	9	
Number of Peaks Remaining to find	5	
Number of Reversals/Recycles remaining	1	
Present Collection Status	In the delay period before valve switch...	

Figure 2-11. An example screen that might be seen by the user during an experimental run.

For this thesis, data files were copyed onto 3.5", high density floppy disks for use in a Macintosh SE/30. The files were converted to Macintosh format through the use of a high density Macintosh floppy drive (SuperDrive™) and a software program called Apple File Exchange. Once converted, the data were then entered into a Macintosh numerical/statistical/graphing program called Kaleidagraph™. This program allows for standard curve-fitting, user entered curve-fitting equations, the determination of peak area using selected starting and ending points, and various statistical functions.

6. Other Programming Considerations

a. Peak Detection

One of the main considerations of this program is how to determine when a peak has passed through the detector. This problem was solved by the use of a threshold value (see Figure 2-9). As previously mentioned, the user is asked to input a threshold value upon which the start and end of a CFA peak is to be determined. After the first 10 points of the run are collected, the average value of the first three points is compared to the average value of the last three points. That difference is then compared to the threshold value. If the difference is greater than the threshold value, then the peak has started. If the difference is less than the threshold value, then the process is repeated again with points 2, 3, 4 and points 9, 10, 11. Using the first three points and the last three points in a string of ten points also eliminates the problem of noise causing the start of a peak. If the threshold is set low, however, this can still be a problem. The other advantage of this method is that it uses the slope change in the CFA peak to

determine the start of the peak, and not just a decrease in voltage. This helps to discriminate against source drift.

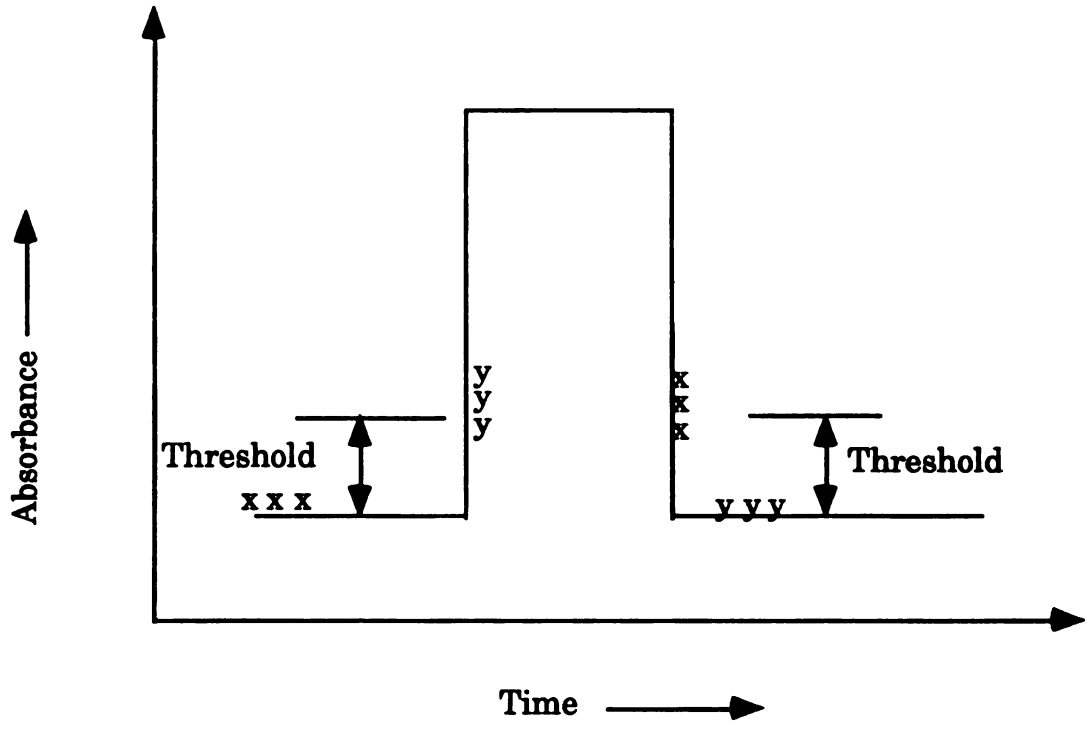

Figure 2-12. The threshold value is determined using the difference between the first three points and the last three points in a 10 point series. When the threshold is large enough, the beginning of the peak is "determined". The end of the peak is determined in the same manner, only the difference must also be near the initial value used when determining the start of the peak. The "x" represents the first three points and the "y" represents the last three points in a series of 10 points.

To determine the end, the absolute difference is taken continually along the CFA peak and compared to the threshold. If the difference is sufficient, then a second condition must be met. That condition compares the average of the first three values (which would be the last points coming down the tail of the peak) to the average of the first three values that determined the start of the peak to some preset range. Detecting the tail in this manner ensures that the peak returns to near baseline, and prevents premature endpoint determination.

b. Valve Switching

Valves are switched by using TTL signals generated by the RTI-815 data acquisition board at the appropriate times. Each TTL signal is sent to an Opto-22, which converts the RTI signal to light, and then the light triggers a relay that operates solenoids, which then control pneumatically actuated, 6 port valves.

c. Delay Times

The delay time between the detector and valve 2 is a predetermined number of points. For example, if the last point that determined the end of the peak was point 115 and the delay time is 15 points, then the valve(s) will switch after point 130 is detected. This procedure actually gives a 30 point line between peaks, which provides ample time to get a flat baseline between peaks. The delay time when doing recycles is actually the amount of time that will take the sample to go completely from coil 2 to coil 1, as calculated from user entered variables.

Chapter 3

Characterization of the Flow Reversal/Flow Recycle System

A. Overview

This chapter covers the characterization and performance of the Flow Reversal/Recycle CFA system. Experiments investigating the influence of different numbers of reversals and recycles on peak shapes (areas and heights) are described. A phenol red/borax buffer is used as the sample. Second, the analytical performance of the new system is compared with the analytical performance of a typical CFA system using the analytical determination of nitrite by the Griess Reaction (27). Finally, the interaction or carryover is determined for a multiple number of valve switches. Finally, the performance of the peak detection routine is evaluated using data from the Griess reaction.

B. Experimental

1. Reagents for the Dispersion Experiments

a. Borax Buffer

The borax buffer was prepared by adding 3.800 g of borax to 1 L of distilled water. The pH was adjusted to 9.5 using 50% NaOH. The solution was then filtered and Brij-35 was added.

b. Phenol Red Dye

The dye was made from a 5.0 mL dilution of phenol red with the borax buffer from a 1.0 mM/0.001 M NaOH basic dye solution and then filtered.

2. Reagents for the Nitrite determination

a. $NaNO_2$ stock solution

0.1725 g of dried $NaNO_2$ was diluted to 500 mL using distilled water. The solution was filtered and then, from the stock solution, 2.5, 5.0, 10.0, 15.0, and 20.0 μM dilutions were made. These solutions were stored in glass bottles and refrigerated.

b. Sulfanilamide (SAN)

SAN was prepared by adding 5.000 g in 250 mL of water, plus 100 mL of concentrated HCL in a 500 mL volumetric flask. The HCl is added to attain the proper solution pH. The solution was filtered, and then one milliliter of Brij-35 was added and the solution was stored in an amber bottle and refrigerated.

c. N-(1-Naphthyl)ethylenediamine dihydrochloride (NNED)

NNED was made by the addition of 0.5000 g of NNED diluted to 500 mL using distilled water, filtered, and then stored in an amber bottle and refrigerated.

C. Instrumentation

All instrumentation, computer control and data acquisition techniques are the same as previously described in Chapter 2. Specific pump configurations and manifold designs will be detailed during the introduction to each experiment.

D. Peak Shape Determinations

1. Introduction

After the construction of new instrumentation, it is necessary to characterize the system. Because the performance of CFA systems have been previously well characterized in regards to the effects of flow rate, coil length, etc., on peak shape, and the new system is essentially a traditional CFA system with valves inserted into the flow path, it follows that those same effects should hold for the flow reversal/flow recycle system. As a result, the experiments performed were primarily concerned with the effect of valve switching on the peak shape.

The first set of experiments were performed using a phenol red/borax buffer dye system that absorbs at 540 nm. Sample and wash times were 20 and 20 seconds, respectively, as recommended by Patton (27). Pecking during sample introduction was used to help minimize dispersion across the pump. The pump and manifold configurations are shown in Figure 3-1. The configurations were the same for both the flow recycle and the flow reversal experiments, with only the connections to the valves being changed (as described in Chapter 2). Trials were run for 1 sample and multiple valve switches, two samples and multiple switches, and finally three samples and one valve switch. The results were used to determine what effect the valve switches had on peak area and peak height.

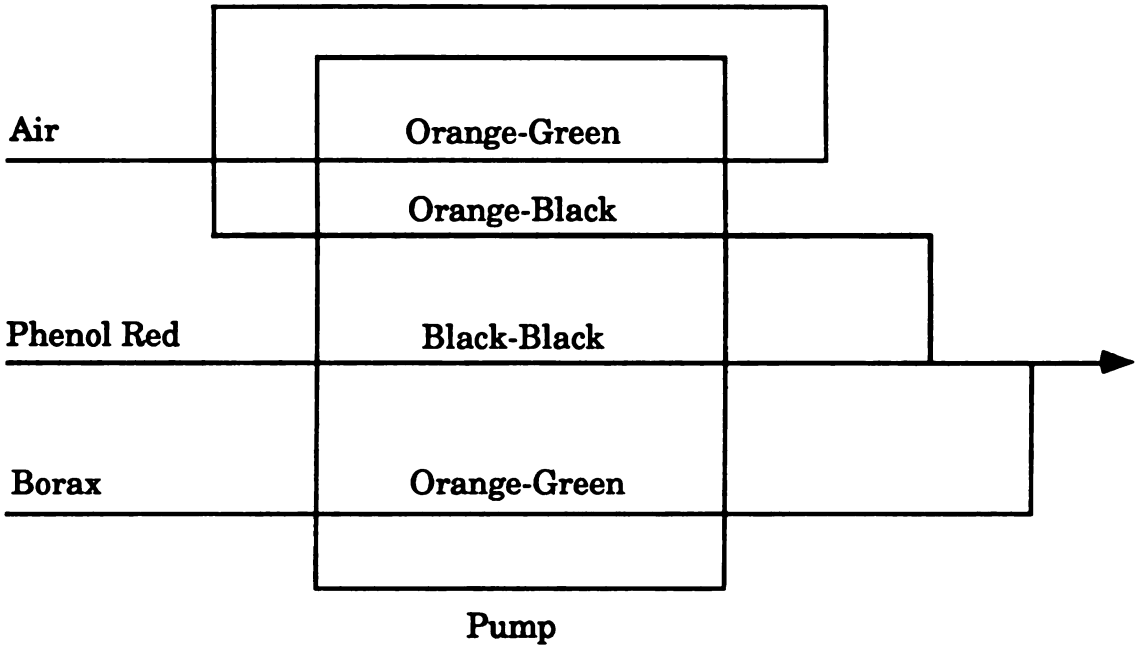

Figure 3-1. The pump configuration and tubing selections for the manifold used to study the effect of valve switching on peak shape using a phenol red/borax buffer system.

2. Influence of Valve Switching

At the outset of this project, there was concern as to what effect switching valves was going to have on a flowing stream. If the switching caused turbulence problems it would significantly degrade the peak shape and peak area (significantly degraded being roughly a 5-7% difference between the original peak and the peak detected after a switch). This degradation would cause the current project to have significant problems. Fortunately, this was not the case. The influence of valve switching on peak area and peak height is shown in Figures 3-2 and 3-3. From these figures, it can be concluded that valve switching does not significantly change the peak shape in terms of peak height and peak area. Therefore, this type of method could be useful for analytical work. Examples of output from the reversal/recycle apparatus are given in Appendix A.

Examining these two figures closely, one can see that, as with typical CFA systems, the peak area and peak height change the longer the sample is in the system. This is as predicted by Snyder's model. The fact that the peak area is changing both in the positive and negative directions indicate that the sudden change in pressure is having some sort of effect on the stream, most likely compressing or expanding the air bubbles, which would make the sample segment of the flowing stream either spread out or condense. As such, the area of the peak either rising or falling, depending on whether or not the bubble is being expanded or condensed.

Consider first peak height from Figure 3-3, peak height changes by approximately 3% over the course of 4 to 5 valve switches. These variations can be due to a number of instrumental parameters, most notably source drift. Also, notice that the increase in peak height appears to level off around 3% after the fourth reversal or recycle, which would indicate that

this variation in peak height is probably a limitation of the instrumentation.

Dispersion values for the reversal and recycle peaks were obtained using a graphical estimation method (9,27). They are presented in Table 3.1. The values do not follow a linear increase with time, probably due to the momentary change in flow rate and pressure introduced into the system during a valve switch. These changes make dispersion prediction difficult, as evidenced by the difference between values predicted by Snyder's equation. The important aspect of the dispersion values is, however, that dispersion is less than three seconds, with is within acceptable limits.

Table 3-1. A comparison of calculated and experimental dispersion values. All dispersion values are in seconds.

Valve Switch	Reversal		Recycle	
Number	Theory	Calculated	Theory	Calculated
0	5.79	0.960	5.79	1.071
1	7.70	2.627	14.24	2.367
2	9.58	2.368	19.27	1.600
3	11.07	1.975	23.09	1.593
4	12.45	2.394	26.34	1.965
5	13.80	2.772	—	—
Average	10.06	2.183	17.75	1.719

Another intriguing possibility for the reversal/recycle system would be if it could be used to analyze more than one sample per run. That is, a user could introduce two peaks into the system and get multiple information on multiple peaks during the same run. Preliminary investigations into this possibility yielded encouraging results. The tricky aspect of this situation is to remember that in flow reversals, the last peak through the detector is the first peak back into the detector when the flow is reversed. With recycles, the peaks always enter the detector in the same order. Preliminary data for this type of analysis are given in Tables 1-4, located in Appendix B.

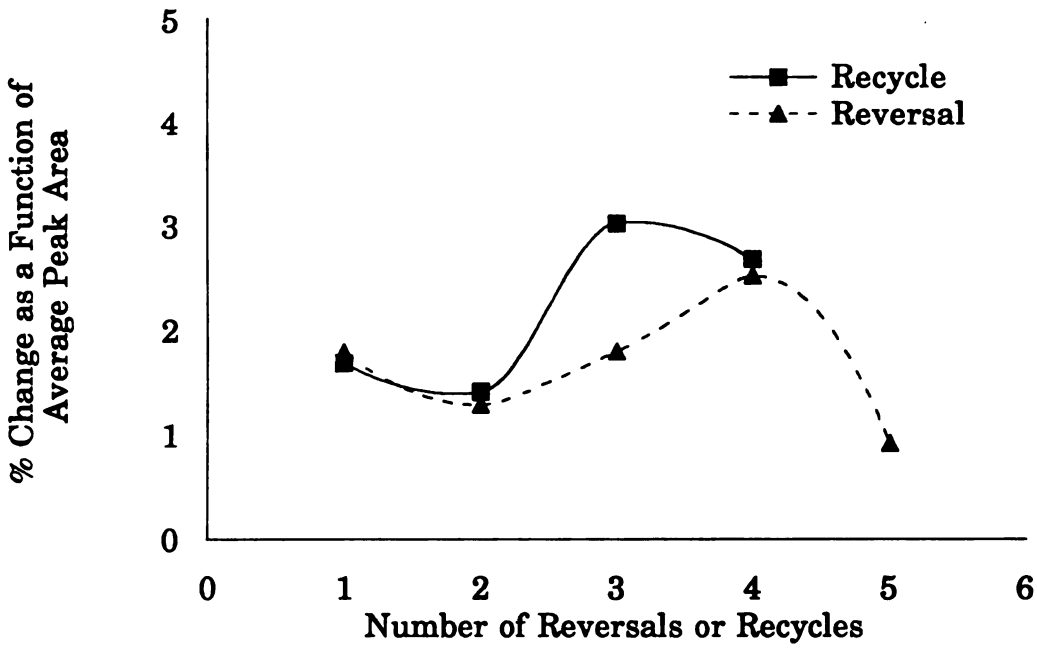

Figure 3-2. The change in peak area as a function of average peak area after each successive reversal or recycle.

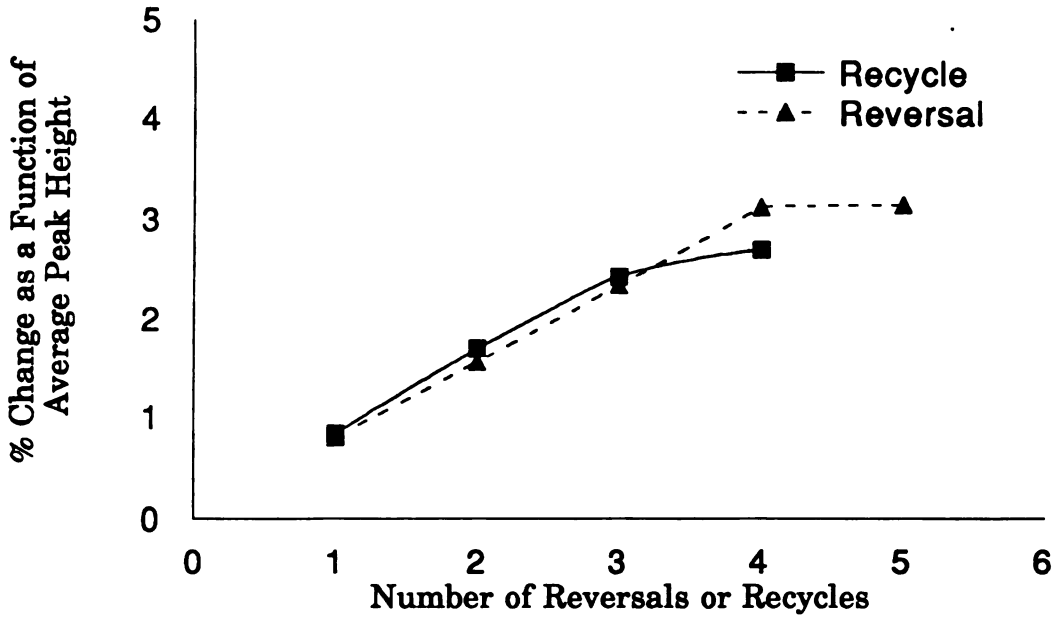

Figure 3-3. The change in peak height as a function of average peak height after each successive reversal or recycle.

E. The Griess Reaction

1. Introduction

In order for the flow reversal/recycle system to be preferred over a regular CFA system, in needs to preform as well or better during analytical determinations. Because of the large amounts of data that can be collected during a reversal or recycle (when compared to regular CFA, it can easily be 3 times more), it may be more precise. For example, in regular CFA, runs are done in triplicate and, as such, three data points are obtained. In reversal or recycle CFA, runs are done in triplicate, but also with two reversals or recycles each time, and, as a result, nine data points are obtained. However, it will also take longer, which is a disadvantage. The amount of sample required will be equal (assuming 3 trials), but the reversal/recycle system will use more buffer. The possibility exists to do 1 trial with two reversals or recycles to obtain three points, but to do this would be risky because something could be wrong with your first sample, and the analyst would get three values for the same "bad" peak and then all of the data would be wrong without the user even realizing the mistake.

The reaction chosen to test the reversal/recycle system is the Griess reaction (27). It is shown in Figure 3-4, and produces a red dye that absorbs at approximately 550 nm. The manifold set up is shown in Figure 3-5. Notice that it uses a ten-turn coil to mix the sample and SAN before NNED is added. A sample time of 20 s and a wash time of 20 s were used, and runs were made in triplicate.

The Griess reaction allows us to examine several aspects of the reversal/recycle system. Using the Griess reaction, a calibration curve is constructed and is compared to the working curve generated using the standard CFA technique (from now on, CFA implies standard CFA, while

reversals or recycles will be specified). In addition to the working curve, an interaction test pattern is obtained by sampling, in this order, 2.5 μM, 20 μM, and 2.5 μM, in accordance with the method of Theirs *et al.* (67). Evaluating the peak widths for differences, and evaluating the time between the end of one peak and the start of the next peak after a valve switch (and thus the consistency of our peak detection routine), are also done at this time.

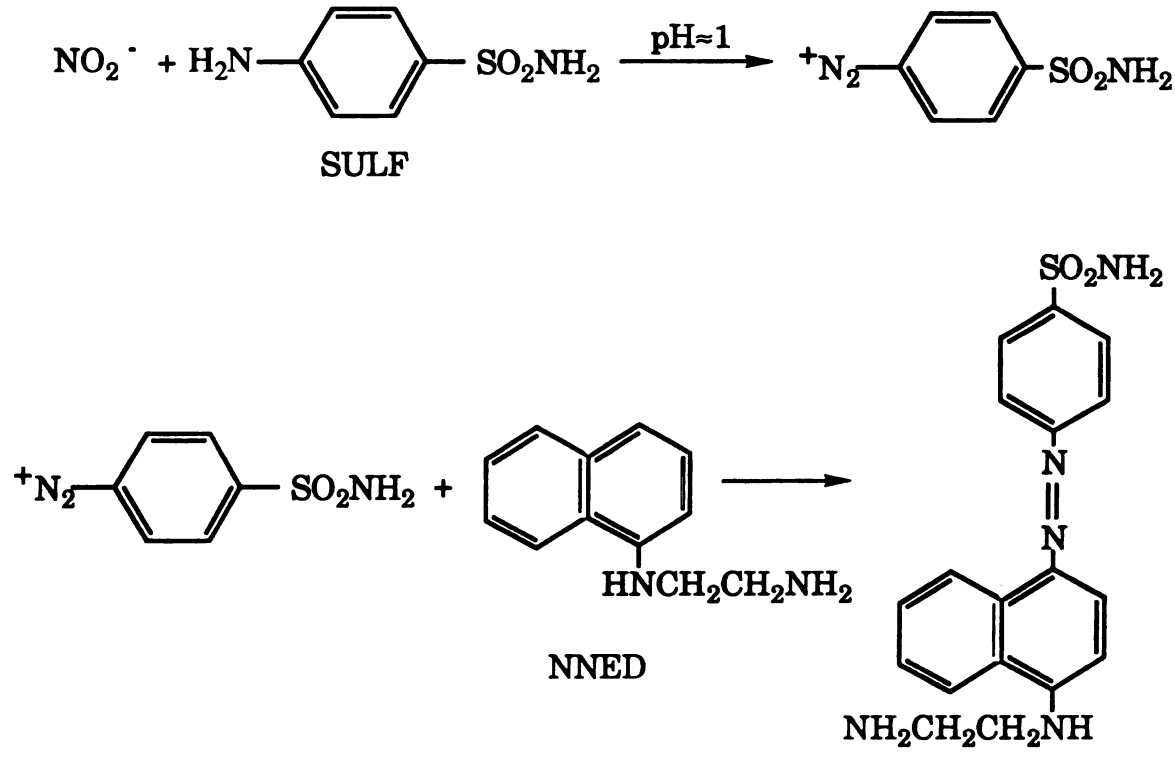

Figure 3-4. The reaction scheme for the determination of NO_2^- using the Griess Reaction.

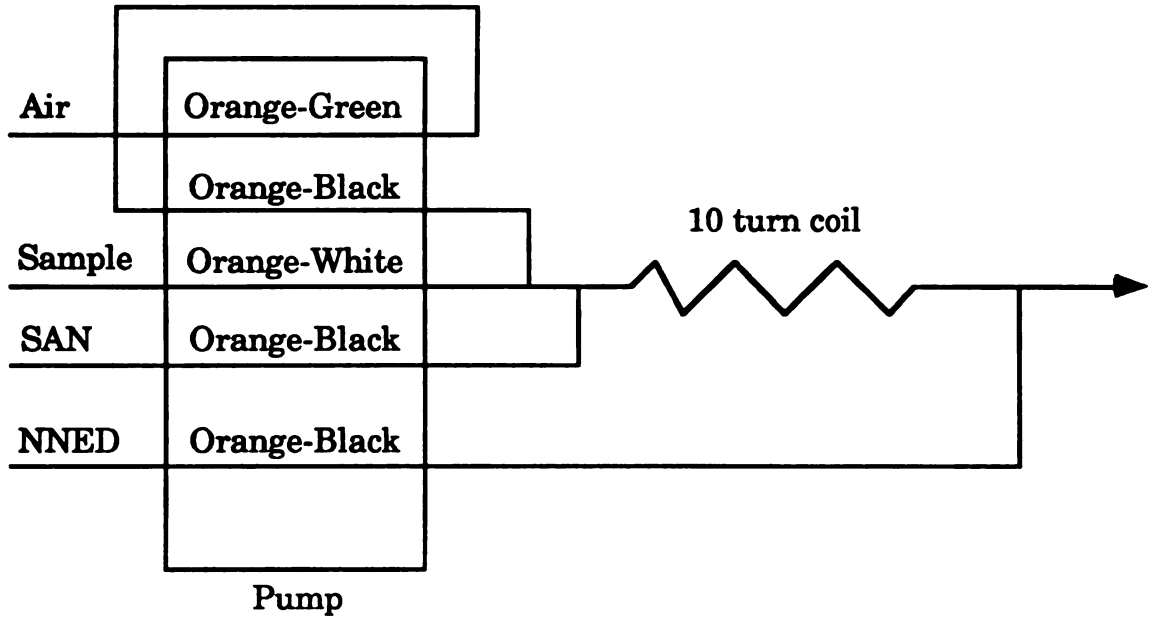

Figure 3-5. The pump configuration and tubing sizes for the manifold used for the Griess reaction.

2. Calibration Curves

The flow reversal/flow recycle system performed reasonably well, but failed to give as high quality of results as did CFA in terms of %RSD. A reason for this might be because the valve switching is having some sort of effect on the peak that is not obvious physically, or is not illustrated through the dye experiments. If the valve switches are having an effect, perhaps by compressing a peak at one time and then letting it expand the next, it would be reasonable to imagine the %RSD could be greater than that for CFA. In addition, because there are more points being taken, there is more of a chance for this error to occur and be detected. One more explanation would be that with the small degradation in peak shape associated with reversals or recycles, and increase in %RSD could be expected. Percent relative standard deviation data are given in Table 3-2, using 2.5 ppm for

comparison. Also given in the table is an example of the within run variations for reversals and recycles. The values under the reversal and recycle columns in the %RSD overall row represent the %RSD for the entire nine peaks (3 trials x 3 peaks each trial) available. The values under the reversal and recycle columns represent the %RSD between the three peaks in each trial.

The standard curves were plotted for both peak area and peak height, and the results are given in Table 3-3. Despite the %RSD's favoring CFA, the plots almost perfectly overlay each other. Therefore, reversal/recycle methods have proved an adequate analytical technique to at least a sensitivity of 2.5 ppm.

Table 3-2. A comparison of % relative standard deviations for 2.5 ppm nitrite solution using CFA and flow reversal/flow recycle CFA. The CFA data was obtained using three trials.

			Reversal			Recycle	
	CFA	Trial 1	Trial 2	Trial 3	Trial 1	Trial 2	Trial 3
%RSD overall							
Peak Area	0.71	2.89 (considering all trials)			2.39 (considering all trials)		
Peak Height	0.02		1.03			0.67	
%RSD within runs							
Peak Area	NA	0.72	4.81	0.81	2.34	8.10	1.98
Peak Height	NA	0.18	0.02	0.03	0.02	0.00	8×10^{-4}

Table 3-3. The figures of merit from the calibration plots of CFA, Flow Recycle, and Flow Reversal using the Griess reaction. Calibration plots are for both the peak area and the peak height.

	CFA		Flow Recycle		Flow Reversal	
	Area	Height	Area	Height	Area	Height
slope	0.615	0.0327	0.623	0.0322	0.620	0.0322
y-intercept	0.134	0.00288	0.100	0.00267	0.103	0.00228
r_{xy}	0.998	0.999	0.998	0.999	0.998	0.999

3. Percent Interaction or Carryover

Because of the number of times a sample is being reversed or recycled, the amount of sample interaction or carryover that might be occurring is very important. This phenomenon occurs as the flowing stream leaves behind sample along the wall of the tube, and all or a portion of the sample is picked up by the next sample plug. Thus, the original sample is decreased from what it should be, and the following sample is increased more than expected. In a reversal or recycle system, this is definitely of major concern.

As mentioned before, samples of 2.5 μM, 20 μM, and 2.5 μM nitrite were run and the percent interaction was calculated by taking the difference between the maxima of the two shoulder peaks, and then dividing by the height of the center peak and multipling by 100.

Results from the interaction test patterns were very encouraging. They are given in Tables 3-4 and 3-5. The percent interaction values are comparable to known CFA systems (27), and do not seem to increase after

each valve switch. A sample interaction output is given in Appendix II for both reversals and recycles.

Table 3-4. The percent interaction for four flow recycles.

Peak Number	Conc. (ppm)	Peak Height	% Interaction	
1	2.5	0.085450		
2	20.0	0.645190	0.149	
1	2.5	0.086410		
				1 RECYCLE
1	2.5	0.086410		
2	20.0	0.645200	0.132	
1	2.5	0.085560		
				2 RECYCLE
1	2.5	0.085568		
2	20.0	0.645250	0.155	
1	2.5	0.086567		
				3 RECYCLE
1	2.5	0.086610		
2	20.0	0.645230	0.161	
1	2.5	0.085572		
				4 RECYCLE
1	2.5	0.085575		
2	20.0	0.645210	0.167	
1	2.5	0.086650		

Table 3-5. The percent interaction for four flow reversals.

Peak Number	Conc. (ppm)	Peak Height	% Interaction	
1	2.5	0.085442		
2	20.0	0.645190	0.156	
1	2.5	0.086448		
				1 REVERSAL
1	2.5	0.086451		
2	20.0	0.645200	0.129	
1	2.5	0.085621		
				2 REVERSAL
1	2.5	0.085621		
2	20.0	0.645190	0.132	
1	2.5	0.086472		
				3 REVERSAL
1	2.5	0.086501		
2	20.0	0.645140	0.132	
1	2.5	0.085650		
				4 REVERSAL
1	2.5	0.085652		
2	20.0	0.645190	0.135	
1	2.5	0.086525		

4. Evaluation of the Peak Detection Routine

All of the nitrite calibration data that has been generated offers a good opportunity to evaluate the peak detection and valve switching routines in the the software that have been written. Recalling that in the peak detection routine it isn't necessary to know exactly when a peak comes through, just a rough estimate, it is interesting to note just how consistent the peak detection routine is at picking the beginning and the end of peaks and keeping a roughly equal length baseline between them. The data are displayed in Figure 3-6. It shows that the majority of the time, the detector keeps the distance between reversal peaks around 38 seconds, which is

correct knowing that wash times are generally around 20 seconds, and there is a 20 point or 10 second delay period between the end of a peak and the valve reversal. It is also correct for the recycle peaks to be around 160 seconds between peaks.

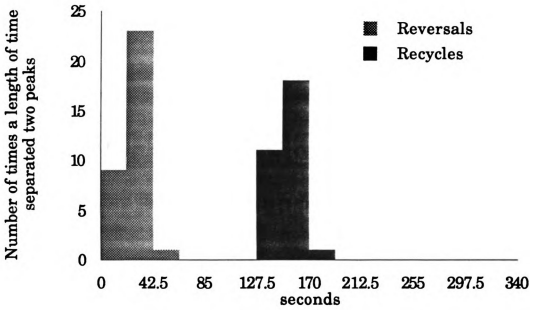

Figure 3-6. A plot representing the frequency of time from the endpoint detection of one peak and the detection of the front of the peak following a valve switch.

Chapter 4

Analysis of the Reaction Rate of Glucose using the Trinder reaction to Investigate the Possibility of Flow Reversal or Flow Recycles being used for the Determination of Reaction Rates.

A. Overview

One of the possible uses of the reversal/recycle system is for the determination of rates of reactions, or kinetics. The problem with current CFA systems is that there is only one point obtained per sample, unless multiple detectors, pumps, split streams, etc. are used. By being able to reverse or recycle a flowing stream, more than one point per sample is obtained. In fact, if the reaction is slow enough, the whole reaction progress curve should be able to be determined. The system developed here has this capability, and it has the advantage of needing only 1 pump and 1 detector. Thus, it is very cost effective, because it doesn't need additional pumps or detectors, and requires very little sample.

This chapter describes the efforts to prove that the reaction rate of glucose with glucose oxidase can be determined with reversals and recycles. The reaction was first performed using standard, single-beam spectrophotometric equipment because it is a competing method. The results of both experiments are discussed.

B. Introduction

The reaction used to compare the reversal/recycle CFA to another analytical technique needs to be slow. Enzymatic reactions are prime examples of reactions whose rate can be easily controlled. The reaction chosen here is the conversion of ß-D-glucose to D-glucono-∂-lactone, or more commonly known as the glucose oxidase reaction. Because the product is not detectable via visible light methods, a detection reaction is needed to form a colored product. The reaction chosen was the Trinder reaction, which has been described previously in the literature (68-71). The product formed is a pink-red dye, which is detected at 510 nm. The reaction is presented in Figure 4-1. The manifold arrangement is shown in Figure 4-2.

C. Experimental

All solutions were the same for both the spectrophotometric experiments and the reversal/recycle experiments. The ratio of the Trinder reagent to the amount of glucose introduced into the system was kept the same throughout; however, the volume of sample was not the same. The experiments used 3 mL of composite reagent and 1 ml of glucose, while the Reversal/recycle system used the same reagents in an approximate 3:1 ratio by employing the proper flow tubes.

1. Buffer

The buffer used was 0.01 M potassium phosphate solution, with a pH of 6.85. This was determined to be the optimum pH for this reaction (71). The solution was filtered, Brij-35 added, and the solution was stored in a plastic bottle.

2. Glucose Solution

A 1000 ppm glucose stock solution was made by mixing 0.5005 g of glucose with distilled water in a 500 mL volumetric flask. The solution was then filtered. Working solutions of 5, 10, 15, 20, 40, 60, and 80 ppm were made using the appropriate dilutions from the stock solution.

3. Glucose Oxidase Enzyme Solution

The enzyme solution was prepared by mixing 0.06 g of glucose oxidase in 50 mL of distilled water. It was made fresh daily and stored at 5 °C.

4. 3,5-dichloro-2-hydroxyphenyl sulfonic acid (DCPS)

A 10 mM stock solution was made from 1.02 g of solid in 0.5 L of distilled water. The solution was filtered, stored in a flask, and refrigerated.

5. 4-aminoantipyrine (AAP)

A 10 mM stock solution of AAP was made from 1.330 g of solid in 0.500 L of distilled water. It was filtered, stored in a stoppered flask, and refrigerated.

6. Composite Reagent

The composite reagent was made by combining 20 mL of buffer, 10 mL of the glucose oxidase enzyme solution, 5 mg of peroxidase, 5 mL of AAP, and 5 mL of DCPS. Brij-35 was added, and then the solution was stored in a stoppered flask and kept out of room light.

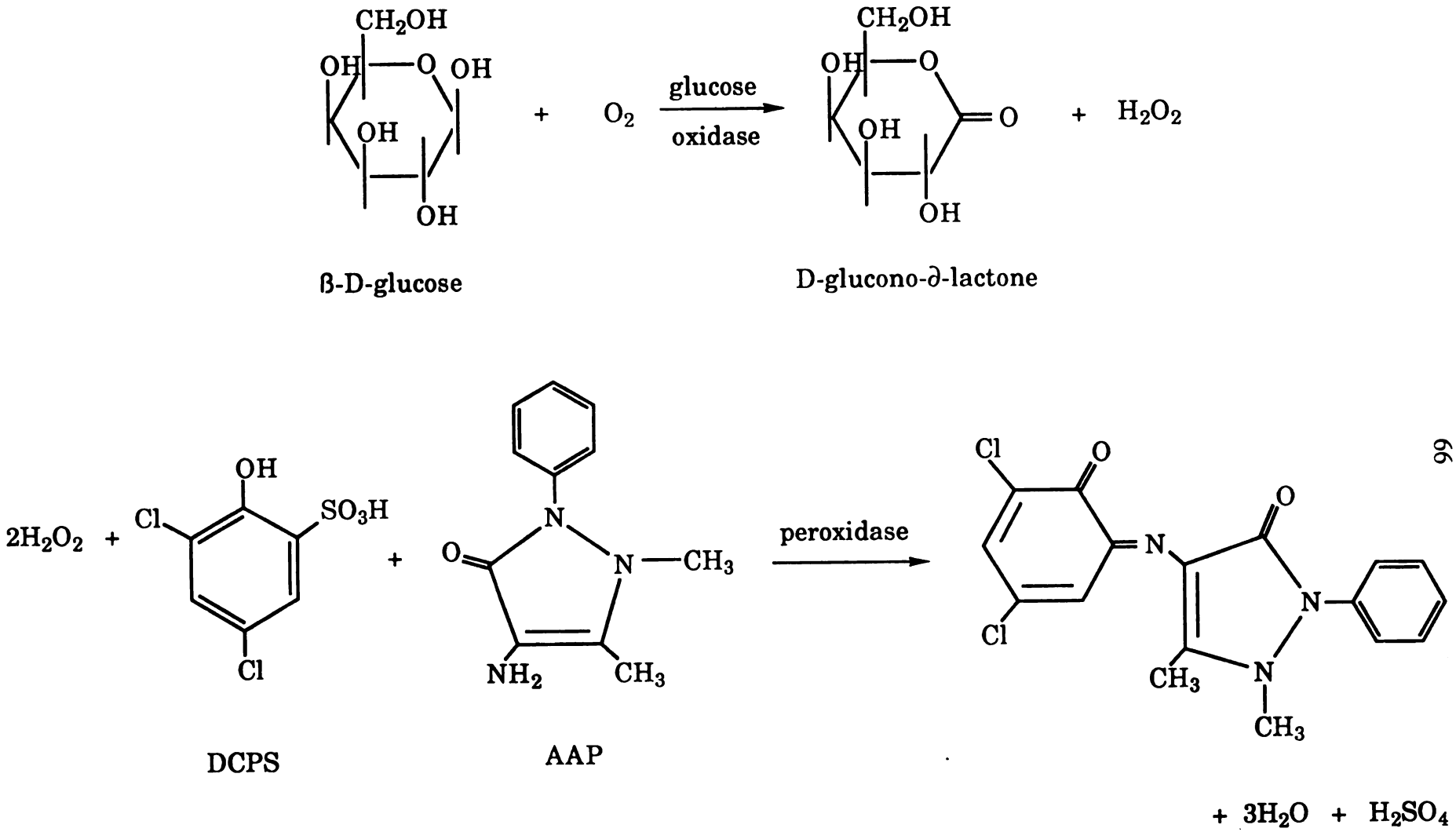

Figure 4-1. The glucose oxidase reaction and the Trinder detection reaction.

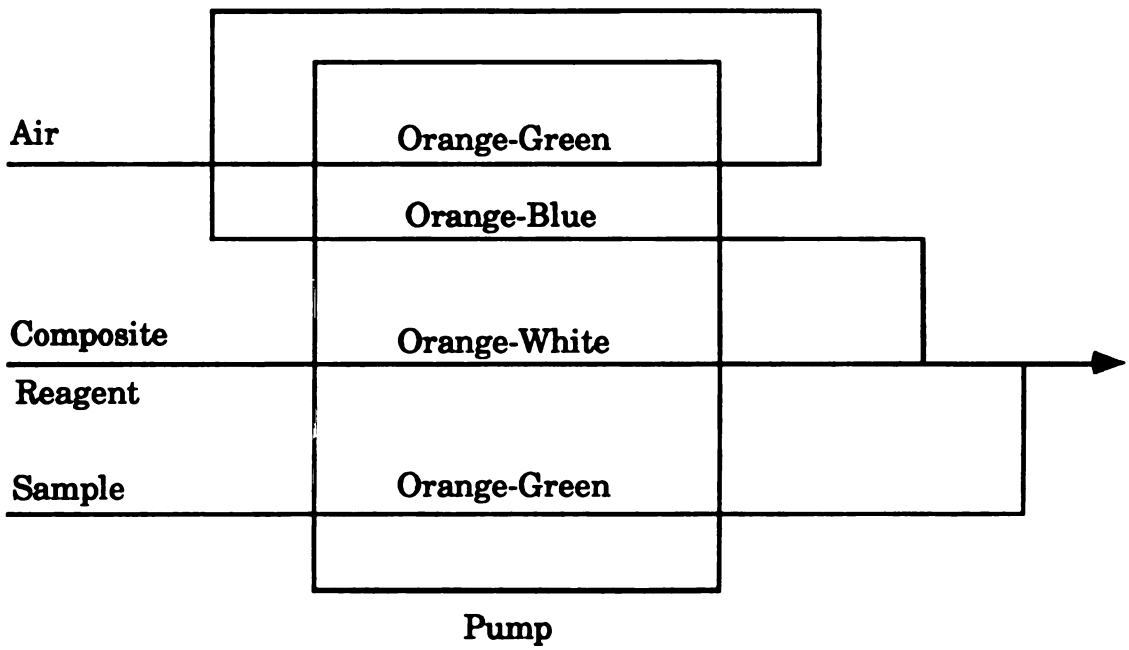

Figure 4-2. The reaction manifold and pump tubing choices for the glucose oxidase/Trinder reaction.

D. Instrumentation

Again, all the reversal/recycle instrumentation is the same. Sample and wash times are 20 seconds each. For the alternate single beam method, the Heath instrumentation was used, and was operated at a slit width of 2 mm and a wavelength of 510 nm. The source was a tungsten lamp. Data taken while using the Heath apparatus were recorded on a strip chart recorder.

E. Results

A relative rate of reaction versus concentration plot for the data obtained from the Heath apparatus is given in Figure 4-3. It was obtained by measuring the rate increase of absorbance over time, after an induction period of approximately 30 seconds. This induction period is important, because it ensures that the rate is being measured during approximately the same time period in both techniques. If the induction period is not considered, the rate for the Heath determinations would be determined in a time frame different than that of the reversal/recycle system, and it wouldn't be a fair comparison. From the plot in Figure 4-3, it is obvious that the linear range for this reaction is between 1 and 50 ppm. It is not linear above 50 ppm because, at high concentrations, enzyme saturation occurs. For this reason, and because any concentration over 20 ppm is kinetically too fast for the reversal/recycle system, only concentrations less than or equal to 20 ppm were used.

The reversal data are very interesting in terms of appearance, and illustrate a problem that will exist when doing kinetics with recycle CFA. Examining Figure 4-4, which is the result of a trial using 5 ppm glucose, notice the shapes of the peaks. The first and third peaks are exactly as is

expected, that is they are flat-topped peaks. The second and fourth peaks are different, and this is because of the first in, last out principle of reversals. With the initial peak, all of the sample volume passes through the detector at exactly the same relative time in terms of when the reaction started. When the sample reverses and enters the detector for the second time, the points on the back of the curve are now on the front and are analyzed first. The points that were on the front of the curve (initially) are now on the back of the curve, and as such have had a longer time to react. Because of this time discrepancy, the peak is no longer flat-topped. It rises from left to right, indicating that the sample towards the back of the sample plug has had more time to react, and thus has a greater absorbance. This is reflected in peak numbers 2 and 4. Interesting to note is that peak number 3 is also flat-topped, but only because the time discrepancy evens out during this reversal. The gives the overall appearance of a flat-topped peak, a spike peak, a flat-topped peak, and then another spike peak.

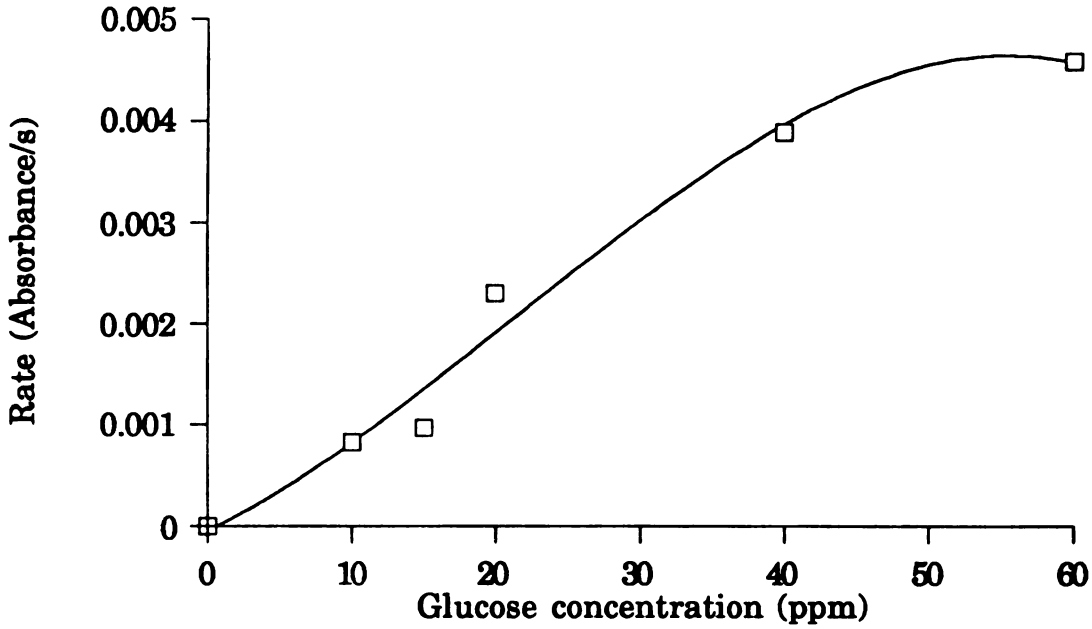

Figure 4-3. The rate of the glucose oxidase reaction using a single beam, Heath instrument.

The recycle data are exactly as expected, giving flat-topped peaks each time because all parts of the sample plug pass through the detector in the time frame during the course of the reaction. This is evidenced in Figure 4-4. An interesting feature in this plot is that the analyst can actually see the reaction slowing down, as evidenced by the peak heights not increasing in a linear fashion after 500 seconds.

To obtain rates for the reversal and recycle experiments, the average peak height and average time during that peak height were obtained for each peak and then plotted. This is illustrated in Figure 4-6 and uses the absorbance versus time data from Figure 4-4. The slope of the linear regression line was taken to be the rate for that concentration. Once the rates for each concentration was known, a relative rate versus

concentration curve could be generated. The regression for these lines, as well as for the Heath experiments, are given in Table 4-1.

Table 4-1. A comparison of the calibration curves for the glucose oxidase/Trinder reaction. The data reflect the linear regression fit to the rate versus concentration data. The units are L ppm^{-1} for the slope and ppm for the y-intercept.

		Reversal		Recycle	
	Heath	Measured	Adjusted	Measured	Adjusted
slope	1.01×10^{-4}	2.60×10^{-4}	1.13×10^{-4}	2.64×10^{-4}	1.15×10^{-4}
y-intercept	-0.0000114	0.000228	—	0.000196	—
r_{xy}	0.98	1.0	—	0.99	—

The results from the reversal and recycle system agree well, but both of the experimental rates are approximately double the rates obtained using the Heath instrument. This is because the ratio of the composite reagent to the glucose sample is different due to limitations in the selection of pump tubing sizes. Once the rate is adjusted for this difference, the rates are similar. There are two possible explanations for the differences between the adjusted reversal/recycle data and the Heath data. One possible explanation for this could be mixing effects. To mix the glucose with the composite reagent during the Heath experiments, a syringe was used. This syringe served two purposes. First, it provided an easy way to inject small volumes of glucose into the spectrophotometric cell. Secondly, by quickly drawing solution back into the sample and then reinjecting it

several times, turbulent flow and mixing is accomplished. This is much better than using a magnetic stir bar, which causes large amounts of noise. In CFA, the mixing is accomplished by coiled tubing inserted after all the components have been mixed together, which provide adequate time for the reaction to go to completion, but also allow for mixing to occur. Secondary flow (bolus flow) is present, and that has been shown to significantly increase radial mixing (29). The differences in rates suggest that CFA provides for increased mixing over the syringe method, and thus a corresponding increase in the reaction rate is seen. Another possible explanation for this could temperature differences. During the reversal/recycle experiments, the reaction temperature was kept at room temperature, but not controlled by a water bath.

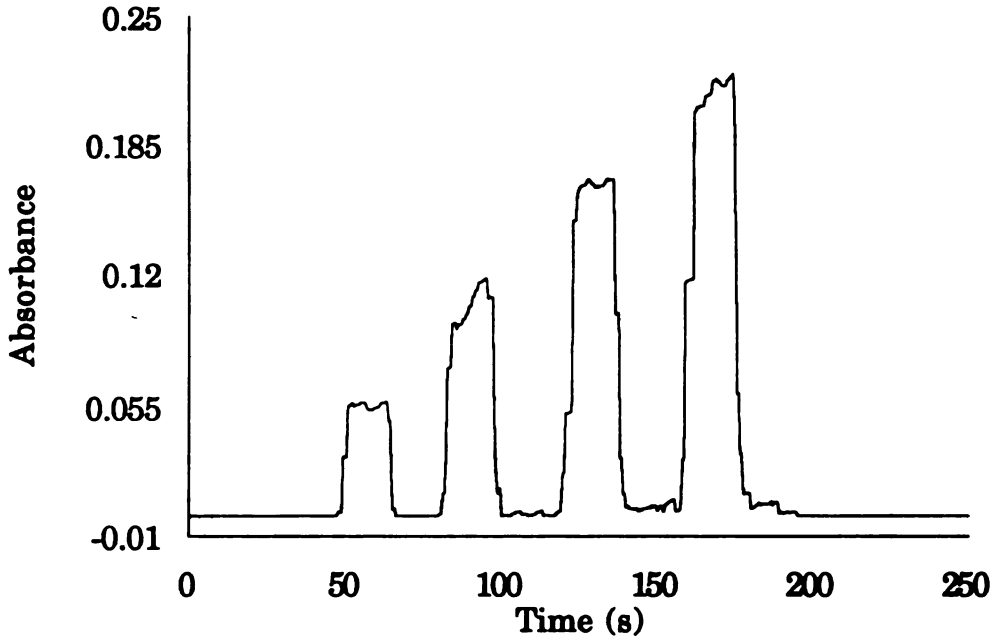

Figure 4-4. An example of the data obtained from glucose oxidase/Trinder reaction using flow reversals.

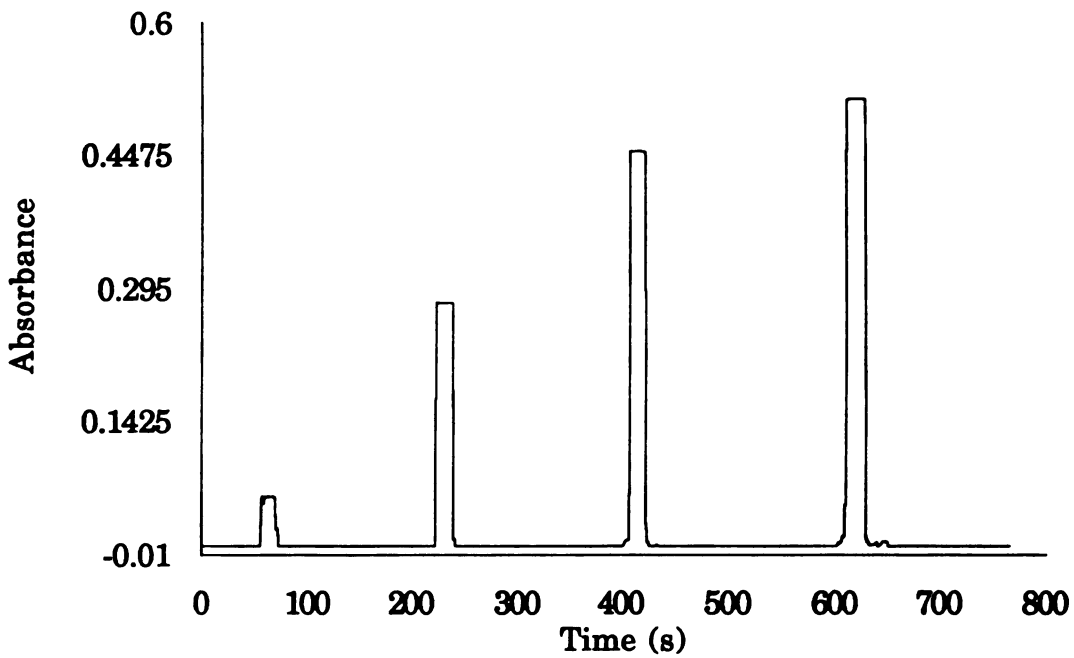

Figure 4-5. An example of the data obtained from glucose oxidase/Trinder reaction using flow recycles.

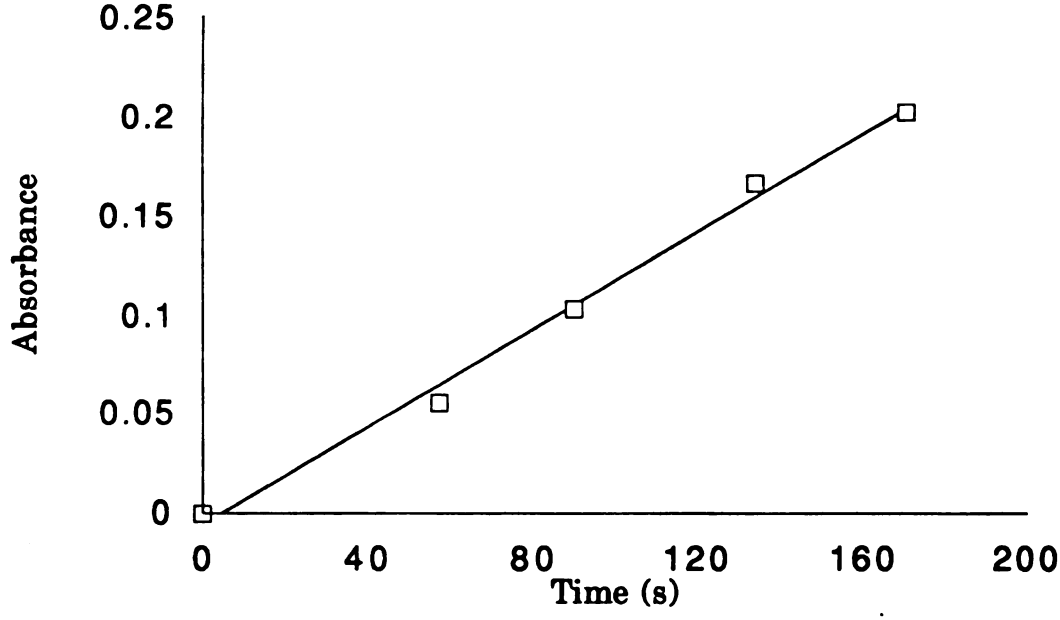

Figure 4-6. The resulting absorbance versus time plot from the recycle data in Figure 4-4.

F. Summary

From the data presented in this chapter, it has been shown that periodic flow reversals or recycles in a CFA system can be used to obtain rates of reactions. This was shown by using the glucose oxidase reaction, coupled with the Trinder detection reaction. Unusual peak shapes were obtained in flow reversals, but can be explained by examining the times at which the absorbances were measured in relation to when the part of the sample stream is passing through the detector. Peaks for flow recycles were flat-topped, as expected. Rate data were obtained from the average peak heights (absorbances) and the average time during the measured peak height, and reasonable rates were obtained. Results were compared to a single beam, Heath instrument, and they varied by about 10%. This difference can be explained by variations in temperature and mixing efficiency.

Chapter 5

Future Projects

A. Overview

The ultimate goal of this project is to create a fully functional, computer-controlled, flow reversal/flow recycle continuous flow analysis system. The system will be able to perform, with just a few modifications in manifold arrangement, coil length, and pump tubing sizes, a variety of regular CFA, CFA Reversal, and CFA Recycle experiments. Also available will be a variety of curve fitting possibilities, statistical functions, and routines to do kinetic analysis. The advantages of such a system would be its inexpensiveness, flexibility, durability, small solution volumes, and ease of usage. It would be applicable to a wide range of slow, kinetic reactions that are not suitable for analysis by such methods as stopped-flow or FIA. These chemical systems are of current interest in this research group and are common to such areas as enzyme reactions or food analysis.

The following projects need to be worked on to accomplish the aforementioned goals.

B. Valve Design

To make flow reversal or flow recycle accessible without changing the valve connections, a new valve configuration has been designed that will allow both reversals and recycles to occur. This new valve

configuration adds a third, 6-port valve to the existing two valves, as shown in Figure 5-1.

The connections during a flow reversal valve switch are diagrammed in Figure 5-2. The flow of the sample is directed through valve a, coil 1, the detector, and then valve b sequentially, as in previous examples (see Chapter 2). After all of the sample has passed through valve b and in coil 2, the flow is reversed by switching only valve a. As a result, the flow is reversed back through valve b and into the detector. The flow should be able to be reversed in this manner several times without significant peak shape deterioration. Similarly, in Figure 5-3, flow recycles can be accomplished by switching valves a, b, and c simultaneously. This will direct the flow through valves c and a, and then into coil 1. Once all the sample is in coil 1, all the valves are switched again, and the sample goes through the detector. A large number of recycles are expected to be available without a large change in peak shape.

The software already written for the flow reversal/flow recycle apparatus provides for the choice of either reversals and recycles in the same program shell, and it would be very convenient if the user could do either method without having to change valve connections.

C. Computer Enhancements

Several improvements in the current system are foreseen. These improvements include, but are not limited to, real-time, graphical output, a full range of curve analysis capabilities, and kinetic routines, in addition to more user friendly utilities.

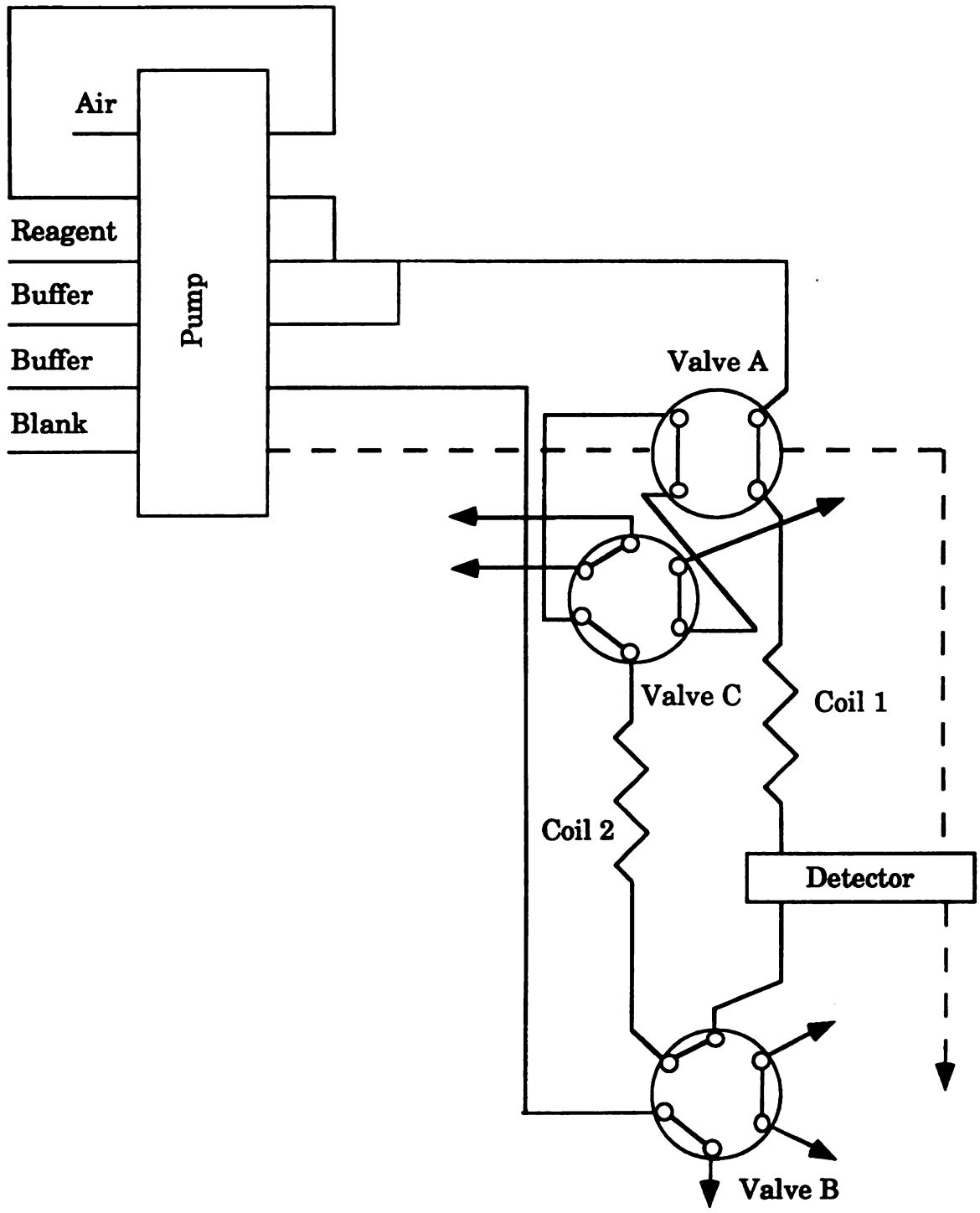

Figure 5-1. The general schematic of the Flow Reversal/Flow Recycle continuous flow system. In this configuration, connections do not have to be switched when choosing between flow reversal or flow recycle modes.

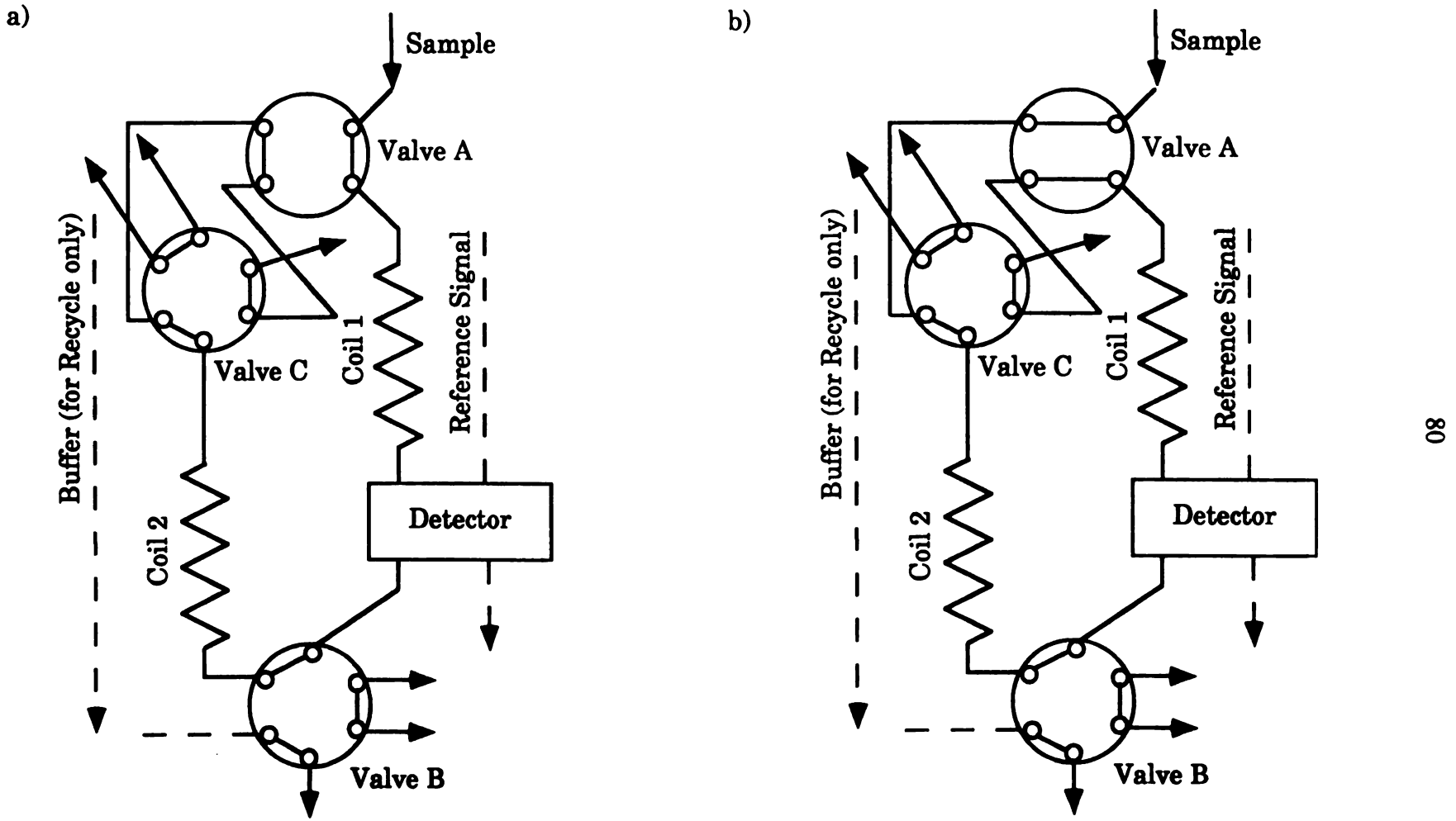

Figure 5-2. The valve configuration for the flow reversal configuration of the Reversal/Recycle valve design. a) shows the initial position while b) shows the valve configuration after a reversal. Notice that in the reversal configuration, valves B and C are stationary. Note: All arrows exiting valves go to waste.

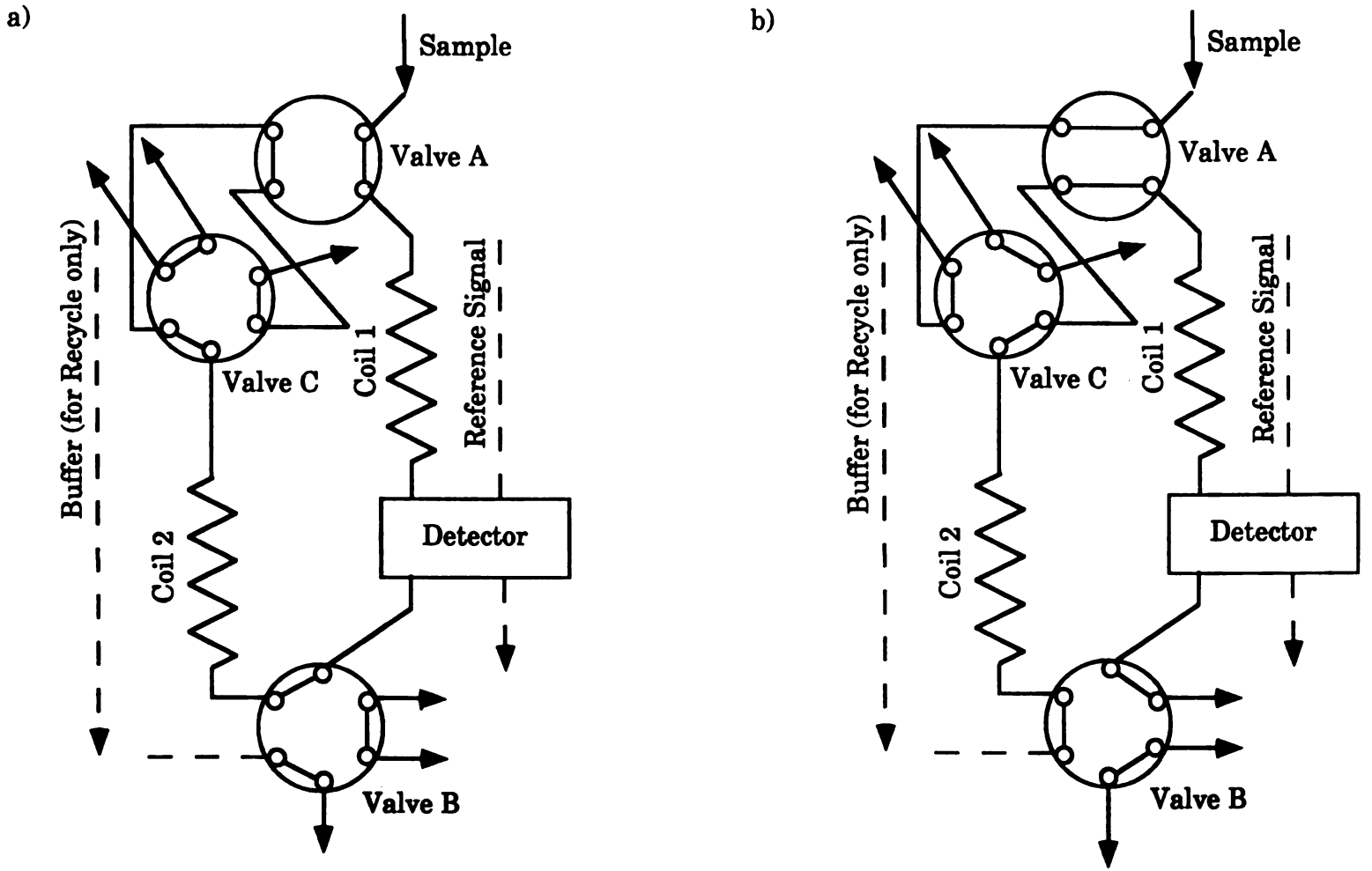

Figure 5-3. The valve configuration for the flow recycle configuration of the Reversal/Recycle valve design. a) shows the initial position while b) shows the valve configuration after a recycle. Notice that in the recycle configuration, all valves are turned. Note: All arrows exiting valves go to waste.

1. Output Screens

One feature currently being investigated is making possible the choice of output screens during the experiment. Currently, the user can only monitor the progress through the use of the chart style output (Figure 2-10). The output format planned would allow for the user to choose either the chart or a real-time, graphical representation of the CFA peak as it passes through the detector. Also, it would be possible for the user to actually be able to cycle between the chart and the graphical output styles whenever desired.

2. Graphing Enhancements

Plans are for the user to be able to select from a wide range of plots, such as a simple voltage versus time plot, a straight absorbance versus time plot, an absorbance versus absorbance plot or various log-log plots. These options will allow the user several different ways to explore experimental data.

3. Peak Analysis

In this area, plans are being made to make peak measurements available immediately after the experiment, as opposed to having to convert data for use in another graphing/statistical program. Needed measurements include peak area, peak height, and a graphical method for estimating dispersion. The user should be able to select the start and end of the data values to be integrated, and to specify or have the computer determine a baseline for reference. The user should also be able to select a region of the continuous flow signal and expand it further (zoom).

Another useful calculation that could be automated would be the sample interaction percentages. These capabilities would allow for improved data analysis, and would let the user have some immediate knowledge of the experimental results. This is in contrast to the present situation, where data are exported to another analysis routine. Any corrections or additional experiments that need to be done have to be done later, which costs the investigator valuable time.

4. Manual Valve Switching

Another useful feature that should be added to the software would allow the user to manually control the valve switching. Currently, the computer has complete control over the valve switching, and the only way a user can interrupt a run is to abort it. Manual control would allow the user to switch valves whenever desired, so features such as quicker and/or slower valve changes or switching in the middle of a peak would be possible.

5. Computer-Controlled Peristaltic Pump

A computer-controlled pump is also planned for this system. This would make investigating the effect of flow rates on chemical systems possible. It would also make stopped-flow CFA, another branch technique of CFA and Stopped-Flow, possible.

6. Computer-Controlled Syringe Pump

Sample introduction is another area where improvements can be made. This research lab owns a syringe pump capable of being computer driven. The syringe pump can deliver small volumes of analyte with great

precision. The addition of the syringe pump would allow for very precise analytical work to be done with any of the CFA system variations that are available.

7. Curve Smoothing and Regeneration

Another area of interest is in curve smoothing and curve regeneration. Patton (27) has shown that these techniques are both useful and possible. Peaks that have been smoothed or regenerated will more closely resemble the curves predicted by Snyder's model, and dispersion calculated from these peaks are very close to predicted dispersion values.

8. Smoothing of Points During Data Acquisition

Currently, the software averages 15 points to make every one point and it is then 1 point on the CFA curve. All 15 points have equal weight when computing the average of that one point. Other smoothing methods, such as the Savitsky-Golay, weight data points in order to their relevance to the point of interest. Points that are close get a large weight, and points that are far away get less of a weight. This might give CFA peaks a better shape and reduce instrumental errors.

D. Segmental Flow Injection Analysis

There has been an interesting paper just published which combines FIA with CFA (72). The authors have designed a special, sample introduction valve which allows them to inject an FIA sample plug into a segmented flowing stream. The result is an FIA plug in a CFA setting, which gives the advantages of both techniques and eliminates some of the disadvantages.

It would be interesting to to try and adapt their valve configuration for the sample introduction to the flow reversal/flow recycle system. This should allow for both FIA reversal and recycle to be done without the dispersion problems that exist in FIA.

E. Kinetics

A major advantage of doing reversal or recycle CFA is the ability to obtain several measurements on the same sample. This is in contrast to normal CFA, which only obtains one steady-state value for each sample sent through the system. Easily envisioned is the ability to take one sample and follow the kinetic curve by reversing or recycling the sample several times. This would allow several points to be obtained for each sample, and a log plot could be generated using the acquired absorbance versus time values. Of course, this system would be applicable only when determining the kinetics of relatively slow reactions.

F. Diode Array Detection

The CFA system should be easily interfaced to the diode array detector in the Crouch laboratory. The diode array can obtain both absorption and fluorescence information nearly simultaneously. The system should be able to monitor mixtures containing several absorbing species, or mixtures containing both chromophores and fluorophores. Being able to reverse a flowing stream through the diode array detection system would allow enormous amounts of information to be obtained in one experiment. This large amount of information would require the use of chemometric techniques for data reduction, smoothing, and analysis.

G. Light Source Modifications

The light source currently used is a Tungsten halogen lamp, which is fine in the visible range, but has some shortcomings when approaching the UV. Specifically, it fails to provide enough light to the detector, starting around 400 nm. In order to do kinetic analysis, frequently a second reaction is needed to form a colored product because the original product formed is not colored. It would be useful to have some UV detection reactions available, such as the conversion of I^- to I_3^-, which is detected at 380 nm. To accomplish this goal, several approaches are available. New diodes that have a larger range could be placed in the detector and a new source module could be built that accommodates a light source different from the current tungsten halogen lamp. Finally, different uses of fiber optics could be investigated, in hopes of trying to get more light to the detector.

H. Other Possibilities

There are certainly a number of other possibilities for this reversal/recycle system. Several samples could be introduced into the system at once, and, thus, several experiments done together. Another possibility would be to introduce a complete working curve and unknown into the system, and then reverse or recycle the peaks several times. Now, in the course of one experiment, several repetitive measurements of the same working curve can be obtained in addition to several measurements of the unknown sample. Also, standard additions could possibly be automated with this system. Thus, precision information is easily measured in one experiment. In addition, the software would be able to plot the curves and determine the absorbance of the unknown sample.

Appendices

Appendix A

The following outputs are given as examples of data for the reversal/recycle CFA system. Output is given for one phenol red dye sample and 5 reversals, one dye sample and 4 recycles, and interaction test patterns for both 4 reversals and 4 recycles.

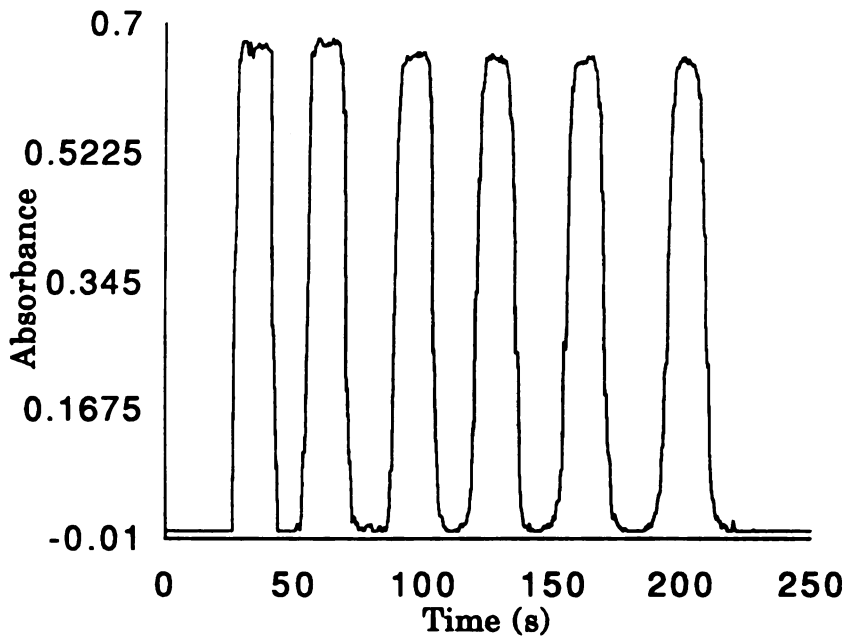

Figure A-1. The output from 1 dye sample with 5 reversals.

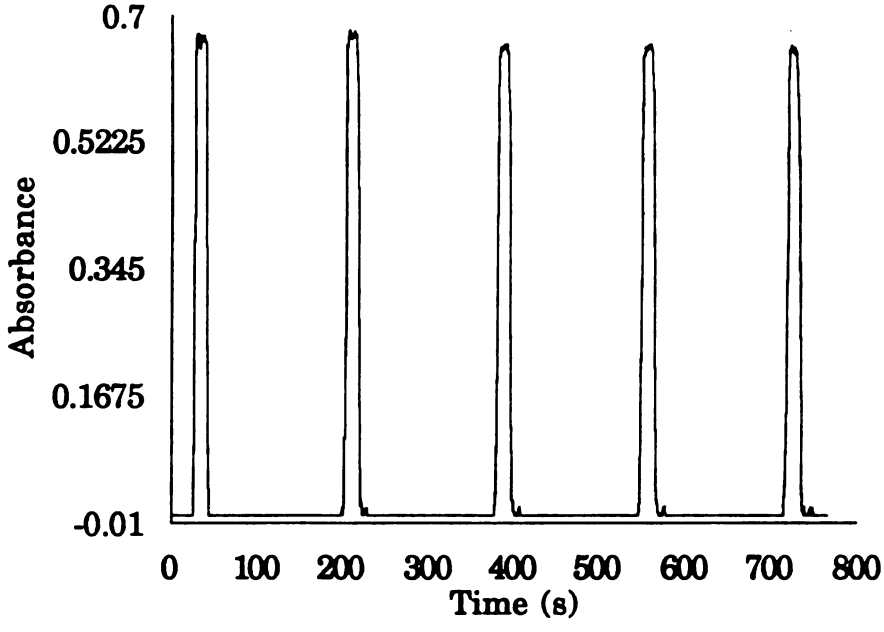

Figure A-2. The output from 1 phenol red dye sample and 4 recycles.

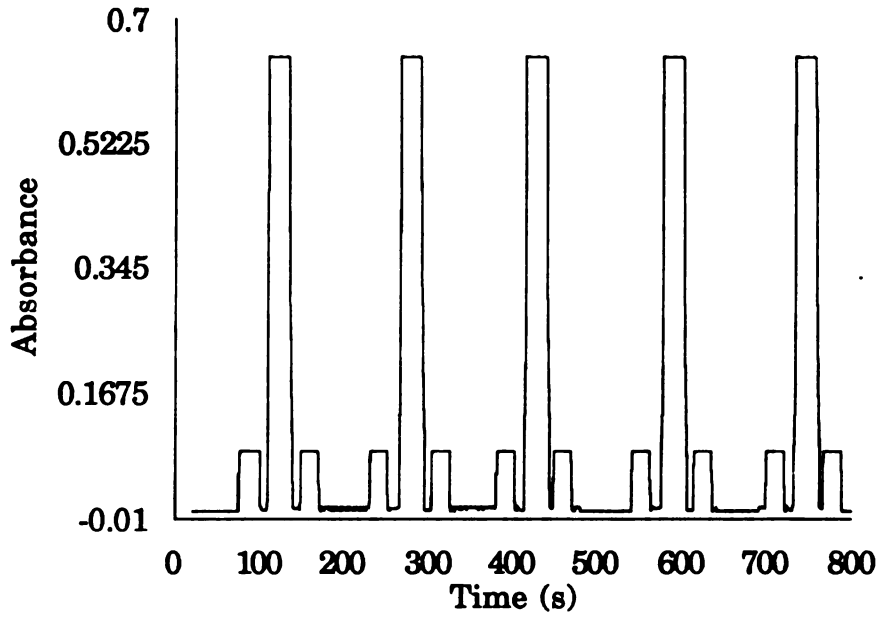

Figure A-3. The interaction pattern for 2.5 μM, 20.0 μM, 2.5 μM nitrite solutions and four reversals.

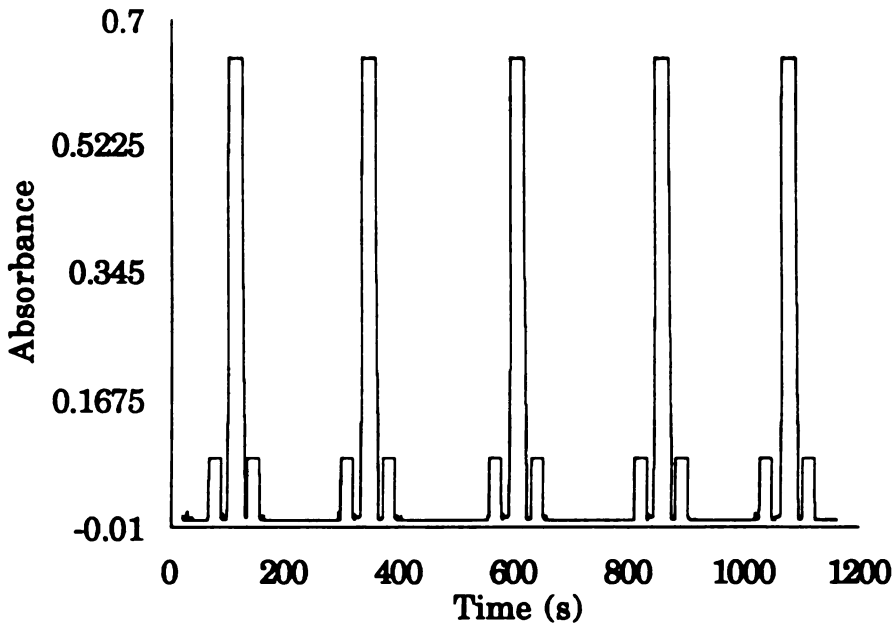

Figure A-4. The interaction pattern for 2.5 μM, 20.0 μM, 2.5 μM nitrite solutions and four recycles.

Appendix B

The following data sheets are for multiple phenol red dye samples and multiple reversals or recycles. It is intended to demonstrate that peak areas and peak shape are relatively constant and that it could be possible to introduce multiple samples and then do reversals or recycles with out peak degradation. These numbers are significant to three decimal places.

The start and stop values are the beginning and end of the peaks, and serve as the limits of integration when determining peak areas. They are measured in seconds.

Table B-1. Data sheet on experiments with 2 dye samples and 2 reversals.

Peak Number	Start	Stop	Start-Stop	Peak Area	(Absorbance) Peak Height
1	21.5	40.5	19.0	10.595960	0.673980
2	52.5	72.5	20.0	10.189880	0.671460
2	85.5	104.0	18.5	10.240660	0.669580
1	116.0	137.0	21.0	10.533750	0.672928
1	150.5	168.5	18.0	10.170370	0.670080
2	185.0	205.0	20.0	10.500690	0.672810
avg			19.4	10.371885	0.671806
std			1.1	0.191810	0.001735
1	41.0	59.5	18.5	10.474760	0.669880
2	73.0	94.5	21.5	10.267410	0.671190
2	108.5	129.0	20.5	10.451450	0.667320
1	148.5	166.0	17.5	10.177910	0.670880
1	183.5	203.0	19.5	10.498650	0.672810
2	219.0	244.5	25.5	10.617030	0.671130
avg			20.5	10.414535	0.670535
std			2.8	0.161683	0.001835
1	25.5	44.0	18.5	10.340980	0.673080
2	54.0	71.5	17.5	10.093030	0.675170
2	86.5	105.0	18.5	10.088930	0.673860
1	113.5	134.0	20.5	10.558850	0.674600
1	150.0	174.5	24.5	10.198370	0.674740
2	180.5	199.0	18.5	10.259850	0.674340
avg			19.7	10.256668	0.674298
std			2.6	0.177056	0.000738
Total AVG			19.9	10.347696	0.672213
Total STD			2.2	0.176850	0.001436

Table B-2. Data sheet on trials with 3 dye samples and 1 reversal.

Peak Number	Start	Stop	Start-Stop	Peak Area	(Absorbance) Peak Height
1	13.0	30.5	17.5	9.861701	0.668990
2	43.5	60.0	16.5	10.058830	0.670520
3	70.5	87.5	17.0	10.480180	0.669790
3	101.0	121.0	20.0	10.527490	0.669780
2	130.0	148.5	18.5	10.298790	0.671430
1	162.0	178.5	16.5	10.137200	0.667410
avg			17.7	10.227365	0.669653
std			1.4	0.256646	0.001372
1	21.0	37.5	16.5	10.058830	0.670520
2	48.0	65.5	17.5	9.861702	0.668990
3	78.0	97.5	19.5	10.191700	0.669720
3	109.0	126.0	17.0	10.473000	0.668990
2	135.0	153.0	18.0	10.297390	0.671430
1	164.0	183.5	19.5	10.191700	0.669720
avg			18.0	10.179054	0.669895
std			1.3	0.207795	0.000943
1	18.5	38.0	19.5	10.191700	0.669720
2	52.0	69.0	17.0	10.480150	0.669790
3	82.0	100.0	18.0	10.058830	0.670520
3	110.5	130.0	19.5	10.058830	0.670620
2	140.0	159.0	19.0	10.060330	0.669785
1	173.0	193.5	20.5	10.164870	0.669726
avg			18.9	10.169118	0.670027
std			1.2	0.163359	0.000423
Total AVG			18.2	10.191846	0.669858
Total STD			1.3	0.209267	0.000913

Table B-3. Data sheet for trials with 2 dye samples and 2 recycles.

Peak Number	Start	Stop	Start-Stop	Peak Area	(Absorbance) Peak Height
1	22.0	39.5	17.5	10.592880	0.674780
2	49.5	67.0	17.5	10.140680	0.672650
1	214.5	233.0	18.5	10.573630	0.669560
2	245.0	266.0	21.0	10.209750	0.673430
1	425.5	446.5	21.0	10.590230	0.669940
2	457.5	477.5	20.0	10.190030	0.672580
avg			19.3	10.382867	0.672157
std			1.6	0.223296	0.002029
1	59.5	80.0	20.5	10.249650	0.670060
2	93.5	112.5	19.0	10.144720	0.672870
1	268.5	286.0	17.5	10.592880	0.673980
2	296.0	313.5	17.5	10.124380	0.671560
1	462.5	483.0	20.5	10.248160	0.670060
2	494.0	514.0	20.0	10.194540	0.671890
avg			19.2	10.259055	0.671737
std			1.4	0.171475	0.001549
1	22.5	43.0	20.5	10.206640	0.669890
2	55.0	75.0	20.0	10.156000	0.672950
1	212.5	232.0	19.5	10.217810	0.669580
2	244.5	263.5	19.0	10.138940	0.672470
1	409.0	429.0	20.0	10.597550	0.673980
2	436.5	455.0	18.5	10.151670	0.672710
avg			19.6	10.244768	0.671930
std			0.7	0.175717	0.001779
Total AVG			19.3	10.295563	0.671941
Total STD			1.3	0.190163	0.001786

Table B-4. Data sheets for trials with 3 dye samples and 1 recycle.

Peak Number	Start	Stop	Start-Stop	Peak Area	(Absorbance) Peak Height
1	13.0	31.0	18.0	9.863906	0.668990
2	50.0	66.5	16.5	10.058830	0.670520
3	86.0	104.5	18.5	10.485520	0.669790
1	219.5	238.5	19.0	9.858550	0.669520
2	258.5	280.5	22.0	10.254940	0.671430
3	294.0	311.5	17.5	10.475310	0.668990
avg			18.6	10.166176	0.669873
std			1.9	0.283883	0.000952
1	13.0	32.0	19.0	10.533150	0.669010
2	55.0	71.5	16.5	10.058750	0.670500
3	92.5	111.0	18.5	10.483210	0.669810
1	228.5	248.0	19.5	10.440220	0.668800
2	270.0	288.0	18.0	10.349320	0.670970
3	314.5	332.5	18.0	10.498720	0.668330
avg			18.3	10.393895	0.669570
std			1.0	0.175962	0.001032
1	15.0	33.5	18.5	9.849703	0.669490
2	54.5	72.0	17.5	10.480900	0.669790
3	98.0	115.0	17.0	10.040630	0.670970
1	223.0	239.5	16.5	10.034720	0.670700
2	264.5	283.0	18.5	10.360750	0.669670
3	302.0	320.0	18.0	10.345290	0.670970
avg			17.7	10.185332	0.670265
std			0.8	0.244944	0.000688
Total AVG			18.2	10.248468	0.669903
Total STD			1.2	0.234930	0.000891

LIST OF REFERENCES

LIST OF REFERENCES

1. Horvai, G. and Pungor, E., *Critical Reviews in Analytical Chemistry*, *17*, 231, **1987**.

2. Skeggs, L.T., *Am. J. Clin. Path.*, *28*, 311, **1957**.

3. Skeggs, L.T., U.S. Patent 2,797,149, June 25, 1957.

4. Ruzicka, J. and Hansen, E.H., *Anal. Chim. Acta*, *78*, 145, **1975**.

5. Stewart, K.K. and Beecher, G.R., Hare, P.E., *Fed. Proc.*, *33*, 1439, **1974**.

6. Stanley, R., *J. Auto. Chem., 4(6),* 175, **1984**.

7. Thiers, R.E. and Oglesby, K.M., *Clin. Chem., 10,* 246, **1964**.

8. Patton, C.J. and Wade, A.P., in *Analytical Instrumentation Handbook*, Ewing, G.W. ed., Dekker, New York, Ch. 27, p 979, **1990**.

9. Furman, W.B., *Continuous Flow Analysis: Theory and Practice,* Dekker, New York, p 61, **1976**.

10. de Jong, E.B.M., U.S. Patent 3,134,263, May 26, 1964.

11. *Practical Automation for the Clinical Laboratory*, White, W.L., Erickson, M.M., Stevens, S.C. eds., C.V. Mosby Company, St. Louis, MO, **1968**.

12. Whitehead, E.C., in *Automation in Analytical Chemistry, Technicon Symposia 1965*, Mediad, Inc., White Plains, NY, p 437, **1966**.

13. Skeggs, L.T. and Hochstrasser, H., *J. Clin. Chem. (Winston-Salem, NC), 10,* 918, **1964**.

14. Smythe, W.J., Shamos, M.H., Morgenstern, S., Skeggs, L.T., in *Automation in Analytical Chemistry: Technicon Symposia 1967,* Vol. I, Mediad, Inc., White Plains, NY, p 105, **1968**.

15. Smythe, W.J., U.S. Patent 3,306,229, February 28, 1967.

16. Lobrig, L.B. and Booth, R.L., in *Automation in Analytical Chemistry: Technicon Symposia 1972,* Mediad, Inc., Tarrytown, New York, p 7, **1973**.

17. Isreeli, J. and Smythe, W.J., in *Automation in Analytical Chemistry: Technicon Symposia 1972,* Vol. I, Mediad, Inc., Tarrytown, NY, p 13, **1973.**

18. Diebler, H. and Pelavin, M., in *Automation in Analytical Chemistry: Technicon Symposia 1972,* Vol. I, Mediad, Inc., Tarrytown, NY, p 19, **1973.**

19. Snyder, L.R. and Adler, J.J., *Anal. Chem., 48,* 1017, **1976.**

20. Snyder, L.R., *J. Chromatogr., 125,* 287, **1976.**

21. Snyder, L.R., in *Advances in Automated Analysis: Technicon International Congress 1976, Vol. I,* Mediad, Inc., Tarrytown, NY, p 76, **1977.**

22. Neeley, W.E. and Sing, H.C., *Am. J. Clin. Chem., 61,* 840, **1974.**

23. Neeley, W.E., Wardlaw, S., Swinnen, M.E.T., *Clin. Chem.* (Winston-Salem, NC), *20,* 78, **1974.**

24. Neeley, W.E., Wardlaw, S., Sing, H., *Clin. Chem.*, 20, 424, **1974.**

25. Neeley, W.E., Wardlaw, S., Yates, T., Hollingsworth, W.G., Swinnen, M.E.T., *Clin. Chem., 22,* 227, **1976.**

26. Patton, C.J. and Crouch, S.R., *Anal. Chim. Acta, 179,* 189, **1986.**

27. Patton, C.J., Ph.D. Dissertation, Michigan State University, 1982.

28. Patton, C.J., Rabb, M., Crouch, S.R., *Anal. Chem., 54,* 1113, **1982.**

29. Snyder, L.R. and Adler, J.J., *Anal. Chem., 48,* 1022, **1976.**

30. Walker, W.H.C., Pennock, C.A., McGowan, G.K., *Clin. Chim. Acta, 27,* 421, **1970.**

31. Thiers, R.E., Cole, R.R., Kirsch, W.J., *Clin. Chem., 13,* 451, **1967.**

32. Walker, W.H.C., *Continuous Flow Analysis: Theory and Practice,* Furman, W.B. ed., Dekker, New York, **1976.**

33. Habig, R.L., Schlein, B.W., Walters, L., Thiers, R.E., *Clin. Chem., 15,* 1045, **1969.**

34. Diebler, H., Pelavin, M., in *Advances in Automated Analysis, Technicon Symposia 1972,* Vol. I, Mediad Inc., Tarrytown, NY, p 7, **1972.**

35. Walker, W.H.C., *Clin. Chim. Acta, 32,* 305, **1971.**

36. Hrdina, J., in *Amino Acid Analysis: 6th Colloquium,* Monograph No. 3, Technicon Corporation, Tarrytown, NY 1967.

37. Theirs, R.E., Reed, A.H., Delander, K., *Clin. Chem., 17,* 42, **1971.**

38. Begg, R.D., *Anal. Chem., 44,* 631, **1972.**

39. Walker, W.H.C. and Andrew, K.R., *Anal. Chim. Acta, 57,* 181, **1974.**

40. Snyder, L.R., Lavine, J., Stoy, R., Conetta, A., *Anal. Chem, 48,* 942A, **1976.**

41. Snyder, L.R., *Anal. Chim. Acta, 114,* 3, **1980.**

42. Rios, A., Luque de Castro, M.D., Valcarcel, M., *Anal. Chem., 57,* 1803, **1985.**

43. Valcarcel, M., Luque de Castro, M.D., Rios, A., Spanish Patent, No. 554725, May 1986.

44. Wade, A.P., Betteridge, D., Crouch, S. R., "Simulation of Flow Reversal FIA for Rapid Automated Speciation and Optimization Sudies", FACSS XIII Conference, St. Louis, MO, October 2, 1986.

45. Rios, A., Luque de Castro, M.D., Valcarcel, M., *Anal. Chim. Acta, 179,* 463, **1986.**

46. Rios, A., Luque de Castro, M.D., Valcarcel, M., *J. Chem. Educ., 63,* 552, **1986.**

47. Wade, A.P., Stults, C.L.M., Crouch, S.R., "Flow Reversal FIA--Muses on Uses", FACSS XIV Conference, Detroit, MI, 1987.

48. Rios, A., Luque de Castro, M.D., Valcarcel, M., *Talanta, 34,* 915, **1987.**

49. Betteridge, D., Oates, P.B., Wade, A.P., *Anal. Chem., 59,* 1236, **1987.**

50. Rios, A., Luque de Castro, M.D., Valcarcel, M., *Anal. Chem., 60,* 1540, **1988.**

51. Toei, J., *Analyst, 112,* 1565, **1987.**

52. Toei, J., *Analyst, 113,* 475, **1988.**

53. Toei, J., *Talanta, 36,* 12, **1989.**

54. Fernandez, A., Luque de Castro, M.D., Valcarcel, M., *Anal. Chim. Acta, 193,* 107, **1987**.

55. Fernandez, A., Luque de Castro, M.D., Valcarcel, M., *Anal. Chem., 56,* 1146, **1984**.

56. Fernandez, A., Luque de Castro, M.D., Valcarcel, M., *Analyst,, 112,* 803, **1987**.

57. Ruz, J., Rios, A., Luque de Castro, M.D., Valcarcel, M., *Fresenius' Z. Anal. Chem., 322,* 499, **1985**.

58. Rios, A., Luque de Castro, M.D., Valcarcel, M., *Anal. Chem., 58,* 663, **1986**.

59. Dahl, J.H., Espersen, D., Jensen, A., *Anal. Chim. Acta, 105,* 327, **1979**.

60. Espersen, D. and Jensen, A., *Anal. Chim. Acta, 108,* 241, **1979**.

61. Hooley, D.J. and Dessy, R.E., *Anal. Chem., 55,* 313, **1983**.

62. Ruz, J., Rios, A., Luque de Castro, M.D., Valcarcel, M., *Talanta, 33,* 199, **1986**.

63. Habig, R.L., Schlein, B.W., Walters, L., Thiers, R.E., *Clin. Chem., 15,* 1045, **1969**.

64. Amador, E., *Clin. Chem. (Winston-Salem, NC), 18,* 164, **1972**.

65. Stults, C.L.M., Michigan State University, unpublished work (1985).

66. Bowman, L.E., Michigan State University, unpublished work (1987).

67. Theirs,R.E., Meyn, J., Wilderman, *Clin. Chem., 16,* 832, **1970**.

68. Trinder, P., *Ann. Clin. Biochem., 24,* 6, **1969**.

69. Barham, D. and Trinder, P., *Analyst, 97,* 142, **1972**.

70. Stults, C.L.M., Ph.D. Dissertation, Michigan State University, 1985.

71. Thompson, R.Q., Ph.D. Dissertation, Michigan State University, 1982.

72. Tian, L.C., Sun, X.P., Xu, Y.Y., Zhi, Z.L, *Anal. Chim. Acta, 238,* 183, **1990**.